QUARTERLY REPORT

ON

LONG ENDURANCE UNDERWATER POWER SYSTEM

(July, 1989 to September 1989)

Contract No. N00014-87-C-0335

PREPARED BY
AQUANAUTICS CORPORATION
980 ATLANTIC AVENUE, #101
ALAMEDA, CA 94501

Table of Contents

1. EXECUTIVE SUMMARY

During the last quarter, work was mainly carried out in five areas:

1. Power Source Concepts
2. Power Source Experimentations
3. Optimization of the ALWATT Batteries
4. Carrier
5. Gill

In cooperation with personnel from Alupower Inc., we have investigated various options to generate power using aluminum as fuel and gill technology to extract oxygen. The advantages and disadvantages of a few of the options were looked into and the energy densities were calculated. The power source scheme, ALWATT-CFFC, under development by Aquanautics can enhance the energy density of ALWATT, an aluminum-seawater battery, to 4000 Wh/l from approximately 2000 Wh/l. This is accomplished by oxidizing H_2 generated from ALWATT in a fuel cell with dissolved oxygen from seawater transported by Aquanautics' proprietary carrier.

In another scheme, the AL-Carrier battery, aluminum is oxidized directly in a battery with the oxygenated carrier. This system is simpler and the energy density could still be higher than the ALWATT-CFFC. But this system has not been developed to any extent. It is to be noted that all these energy density figures are calculated with major assumptions about performance of the systems. In the last quarter a considerable amount of work was carried out in a CFFC and efficiency has been improved to 28% from 18%. Stability of the performance will be checked in the next quarter. Some experiments on the AL-carrier showed feasibility although the long-term performance has not been established yet.

The ALWATT battery which produces hydrogen has been optimized to yield an energy density of about 2000 Wh/l.

Longevity studies with carriers showed that the lifetime of carrier 72 was related to the concentration of free oxygen dissolved in the carrier. The bound oxygen is not responsible for the degradation. Since the free oxygen concentraiton cannot be higher than that in seawater for the gill, the implication is therefore that underwater operation favors the carrier lifetime.

Two membrane cartridges (out of eight ordered) were obtained from AMT and were tested. The cartridges leaked and therefore the results obtained were not reliable. They will be repaired and re-tested. In the meantime, the other cartridges have been procured and will be tested this quarter

2. POWER SOURCE COMPARISONS

2.1 Summary

In this section four possible power source designs utilizing aluminum as fuel are described. Their projected volumetric energy densities were calculated to be about 5 to 10 times that of the lithium thionyl chloride battery. These are tabulated below:

System	Wh/l	Wh/kg	Comments Regarding System Components
Lithium Thionyl Chloride (Li-$SOCl_2$) Battery	430	330	no moving parts
Aluminum Seawater (ALWATT) Battery	2300	1000	no moving parts
Aluminum Dissolved Oxygen (AL-DOS) Battery	2900	1400	seawater pump
Aluminum Carrier (AL-Carrier) Battery	4600	2200	seawater pump carrier pump and gill
Alwatt Carrier Feed Fuel Cell (ALWATT-CFFC)	3800	1900	same as AL-Carrier plus fuel cell

System	Major Assumptions
Al-DOS	37% power efficiency and 30% power consumption by seawater pump
AL-Carrier	47% efficiency
ALWATT-CFFC	57% fuel cell efficiency

These calculations were carried out by Alupower and Aquanautics personnel. Aluminum utilization efficiency in the four schemes is taken to be 80%.

2.2 Introduction

Developing a high energy density electrochemical power source for underwater use requires the following considerations:

1) Energy of reaction
2) Reactants to be carried
3) Ancillary components to be carried
4) Depth
5) Temperature
6) Reliability of the system
7) Endurance required

The following discussion is related to a long endurance (1 - 5 years), 5 - 100 W net output system. For land use one would use a small diesel engine with an occasional fill up of fuel or if cost is of no concern, one would perhaps use the lithium thionyl chloride battery. The lithium thionyl chloride (Li-$SOCl_2$) battery is one of the most powerful primary battery

systems (see Figure 2.1) with energy densities of 1000 Wh/l and 500 Wh/kg[2.1]. Another alternative is to use a SPE fuel cell with methanol reformer or metal hydride as a fuel source. Reference 1 also deals with such options (p. 42.1 - 42.17). The other alternative is the metal air battery. In this case, electrolyte and/or metal must be replaced regularly to ensure a practical system. For long endurance, the fuel cell becomes a very viable system (see Figure 2.2).

On land, the use of a fuel cell has its advantages as the oxidant, O_2, is plentiful in air and one would only need to carry fuel. Under water, this advantage can only be retained if there is an efficient process for harnessing oxygen from seawater. The Aquanautics gill technology development is an attempt in this direction. Because of the presence of seawater, a conducting electrolyte, there are other possible options.

2.3 Options

A power source evolution route started with the Li-$SOCl_2$ (best primary battery) and ended with the ALWATT-CFFC or AL-Carrier battery as shown in Figure 2.3. The systems at the end have approximately 10 times more energy density than the Li-$SOCl_2$ battery.

The five systems that are to be considered are:

A) Lithium Thionyl Chloride Battery
B) Aluminum-Dissolved Oxygen System (AL-DOS)
C) Aluminum-Seawater Battery (ALWATT)
D) Carrier Feed Fuel Cell (CFFC)
E) Aluminum-Carrier Battery (AL-Carrier)

From these, the lithium thionyl chloride battery and the Alwatt are commercially available, perhaps not at the energy density level as given in Figure 2.3. Interested readers are requested to consult published literature or contact the manufacturers (e.g., Altus, San Jose, CA and Honeywell for the Li-$SOCl_2$ and Alupower, Warren, NJ for the Alwatt batteries).

AL-DOS System

In this system, dissolved oxygen in seawater takes part directly in the electrochemical process. Seawater is pumped through the cell housing which constitutes an oxygen-reduction cathode and aluminum anode. The reactions are as follows:

$$2Al \rightarrow 2Al^{+++} + 6e^-$$

$$\frac{3}{2} O_2 + 3H_2O + 6e^- \rightarrow 6(OH)^-$$

$$2Al + \frac{3}{2} O_2 + 3H_2O \rightarrow 2Al(OH)_3$$

The thermodynamic e.m.f. of the above reaction is 2.7 V, but an OCV of 1.4 V is normally observed and on load, the voltage further drops down.

[2.1] Handbook of Batteries and Fuel Cells, ed. David Linden, McGraw Hill, N.Y., 1984, pp. 11-39.

The main disadvantage of this battery is that seawater needs to be pumped through the cell housing (see Figure 2 4). The seawater pump would need about 30% of the power generated according to our estimation. Depending upon the cathode structure, the system may be prone to clogging due to geological fouling and also the hydroxide formation of calcium, magnesium etc on the cathode. Shunt current protections for higher terminal voltage would also be more difficult with this system, as one has to deal with high seawater flow through the battery.

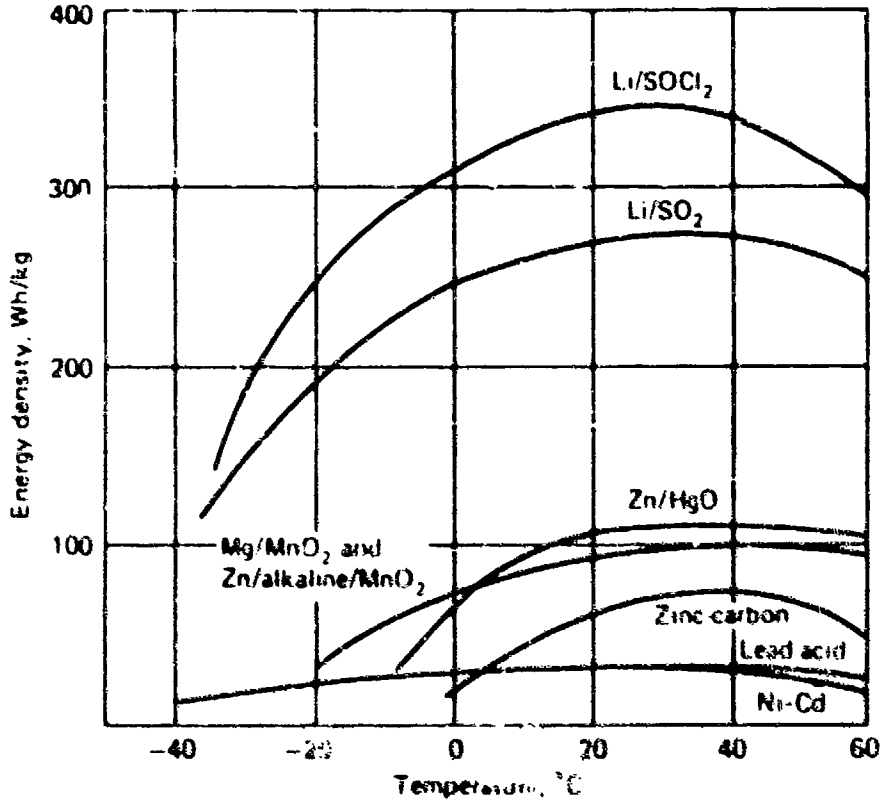

Effect of temperature on gravimetric energy density of primary and secondary cells. Based on D size cells.

Figure 2.1

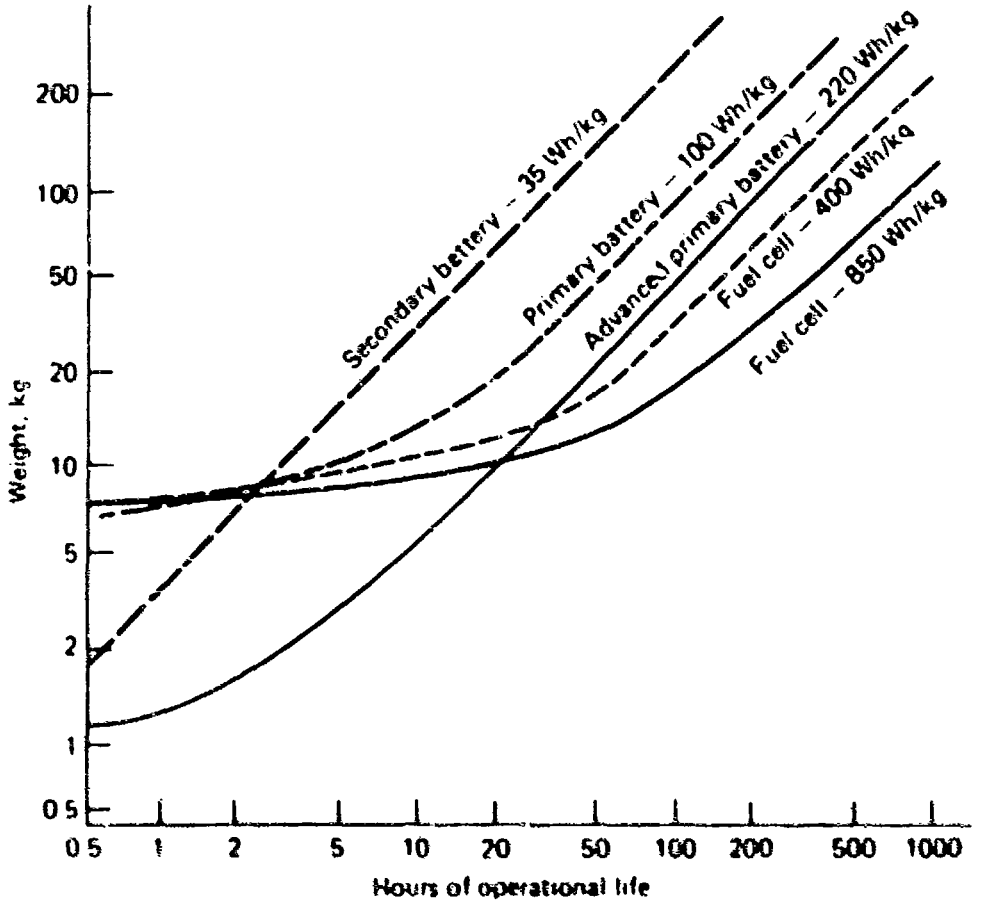

Comparison of electrochemical systems—weight vs. service life (based on 100-W output and stated energy-weight ratio).

Figure 2.2

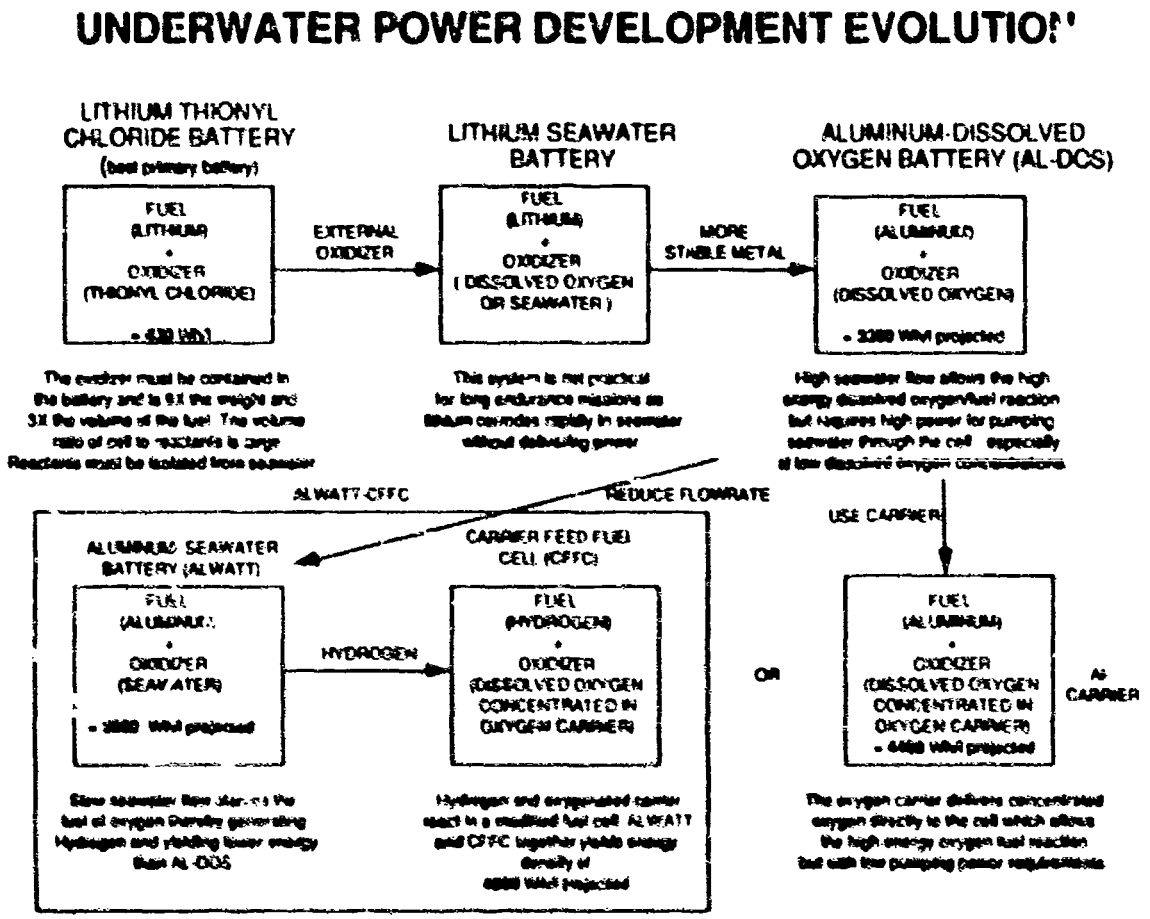
UNDERWATER POWER DEVELOPMENT EVOLUTION
LITHIUM THIONYL CHLORIDE BATTERY
(best primary battery)
FUEL (LITHIUM) + OXIDIZER (THIONYL CHLORIDE)
EXTERNAL OXIDIZER
LITHIUM SEAWATER BATTERY
FUEL (LITHIUM) + OXIDIZER (DISSOLVED OXYGEN OR SEAWATER)
MORE STABLE METAL
ALUMINUM-DISSOLVED OXYGEN BATTERY (AL-DCS)
FUEL (ALUMINUM) + OXIDIZER (DISSOLVED OXYGEN)
ALWATT-CFFC
REDUCE FLOWRATE
USE CARRIER
ALUMINUM SEAWATER BATTERY (ALWATT)
FUEL (ALUMINUM) + OXIDIZER (SEAWATER)
HYDROGEN
CARRIER FEED FUEL CELL (CFFC)
FUEL (HYDROGEN) + OXIDIZER (DISSOLVED OXYGEN CONCENTRATED IN OXYGEN CARRIER)
OR
FUEL (ALUMINUM) + OXIDIZER (DISSOLVED OXYGEN CONCENTRATED IN OXYGEN CARRIER)
Al CARRIER

Figure 2.3

AQUANAUTICS CORPORATION
OXYGEN SYSTEMS

Al - DOS SYSTEM

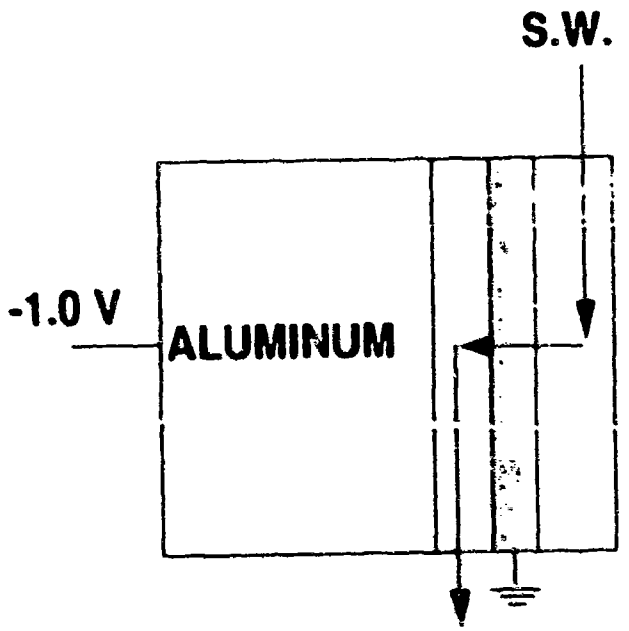

Figure 2.4

With the high oxygen concentration in seawater this system looks very attractive as the amount of seawater to be pumped decreases proportionately. The main advantage is that it is simpler than any of the following processes. It also does not entail any uncertainty of oxygen carrier development.

CFFC

The carrier feed fuel cell is a process being developed by Aquanautics and has been elaborated upon in previous quarterly reports.

AL-Carrier

This scheme is similar to AL-DOS except that the oxygen is carried into the cell by oxygen carrier. Oxygen carrier in turn is supplied with oxygen from seawater through the gill membrane. The advantage of this process is that the oxygen carrier can transport oxygen in a much more concentrated form, so the flow through the cell could be reduced accordingly. Gill design and cell design can therefore be independently optimized to obtain minimum power loss.

There can be two versions of AL-Carrier: direct (Figure 2.5) and isolated (Figure 2.6). In the AL-Carrier direct method, oxygenated carrier comes directly in contact with the cathode. Oxygen reduction produces OH^- ion and the pH of the carrier rises. On the anode side, seawater is the electrolyte which needs to be flown to flush out $Al(OH)_3$ formed. Increase in the cathode pH will reduce the available voltage by 60 mV for each pH unit. The requirement that seawater and carrier do not come in contact with each other leads to the use of the solid anion-exchange membrane. At Aquanautics, there has been some work carried out and it has been determined that pH rises to 12.4 - 12.7.

In the indirect method, the carrier does not touch the cathode and, in fact, it works as a true oxygen transporter. Carrier goes through the cathode separated by solid membrane. The form of solid membrane could be hollow fiber through which carrier flows. This makes the cathode volume large but has the advantage that carrier selection is independent of electrochemistry. In the following discussion this method is ignored in favor of the direct method.

2.4 Detailed Energy Density Calculations

This section describes the calculations which are carried out to obtain system weight and volume for the following underwater energy sources:

1) Lithium thionyl chloride battery ($Li-SOCl_2$)
2) Aluminum seawater battery (ALWATT) produces H_2
3) Aluminum dissolved oxygen (AL-DOS)
4) Aluminum dissolved oxygen via carrier (Al -Carrier)
5) Combination of an ALWATT with a fuel cell utilizing H_2 with oxygen via carrier (ALWATT-CFFC)

This section also describes all the assumptions made in these calculations.

AQUANAUTICS CORPORATION
OXYGEN SYSTEMS

ALUMINUM - CARRIER DIRECT

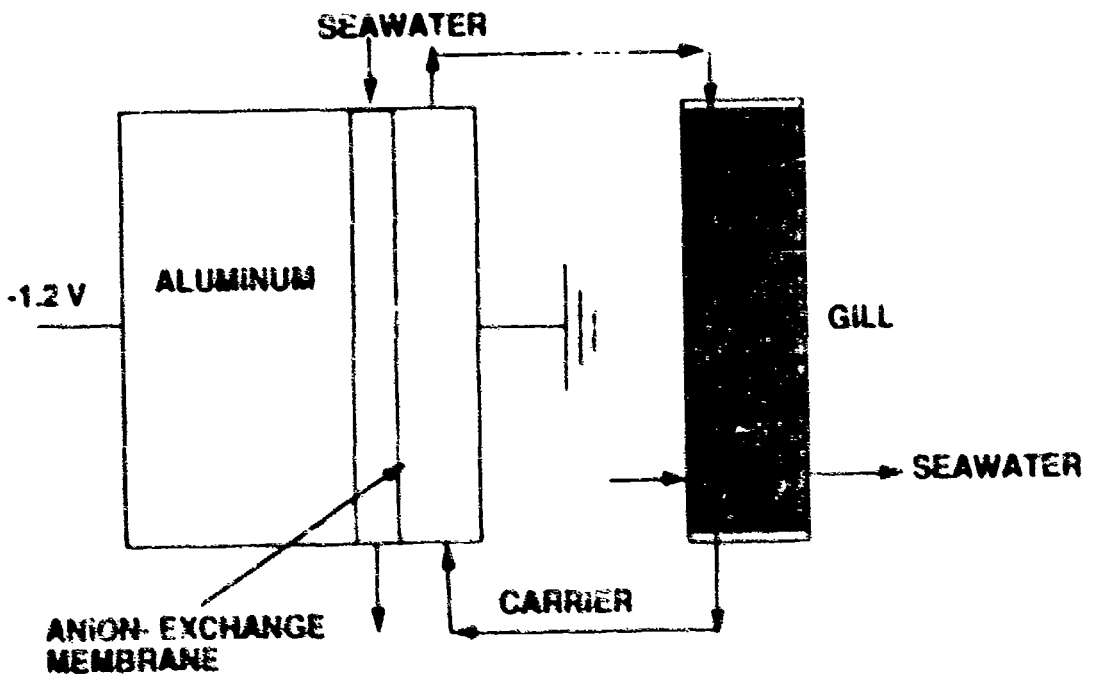

Figure 2.5

AQUANAUTICS CORPORATION
OXYGEN SYSTEMS

ALUMINUM - CARRIER ISOLATED

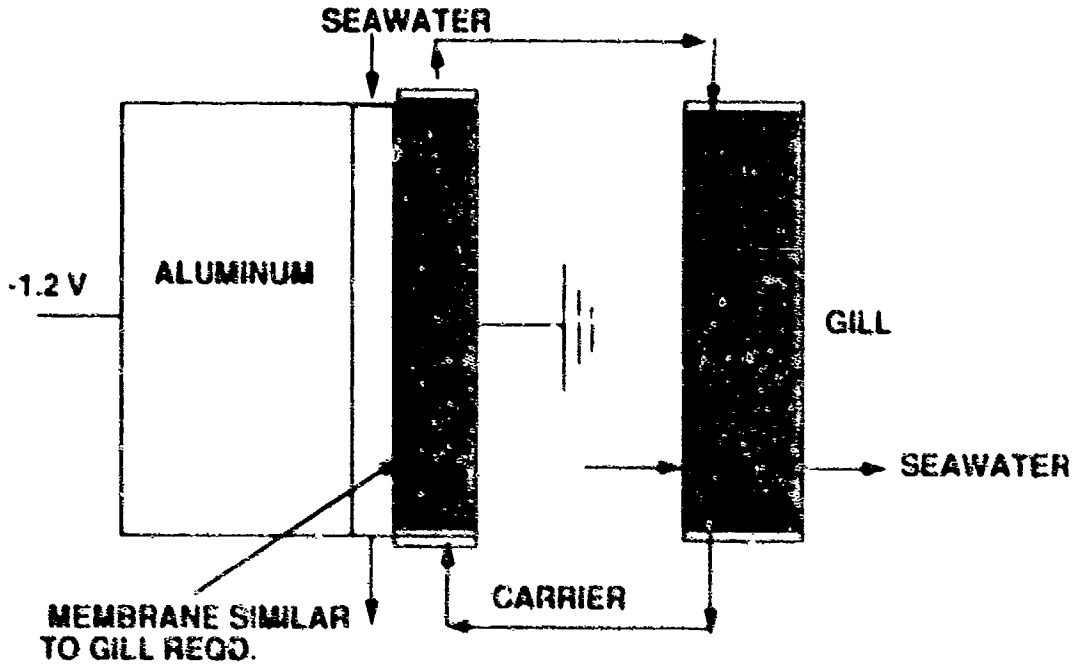

Figure 2.6

2.4.1 Thermodynamic Requirement

The thermodynamic requirement is the minimum requirement of fuel and oxidizer in the energy source. For the above five classifications, the primary fuel, oxidizers and the overall reactions are given in the following table:

	System	Fuel	Oxidizer	Overall Reaction
1.	Li-$SOCl_2$	Li	$SOCl_2$	$4Li+2SOCl_2 \rightarrow 4LiCl+SO_2+S$
2.	ALWATT	Al	H_2O	$2Al+6H_2O \rightarrow 2Al(OH)_3+3H_2$
3.	AL-DOS	Al	O_2(d)	$4Al+3O_2+6H_2O \rightarrow 4Al(OH)_3$
4.	AL-Carrier	Al	$(L\text{-}Co)_2\text{-}O_2$	$4Al+3(L\text{-}Co)_2\text{-}O_2+6H_2O \rightarrow 4Al(OH)_3 + 6LCo$
5.	CFFC	H_2	$(L\text{-}Co)_2\text{-}O_2$	$2H_2+2(L\text{-}Co)_2\text{-}O_2 \rightarrow 2H_2O + 2L\text{-}Co$

Each of these reactions releases energy. If all the energy is converted to useful electrical energy by means of special design and manipulation of the reaction sites (as in a battery, a fuel cell or a combination thereof) the amount of reactants required for a given energy output is defined as the thermodynamic requirement. In reality, it is hardly ever possible to extract all the energy in the form of electrical energy; also, there are components other than just reactants necessary to build a battery. Nevertheless, this is a good place to start since it provides the minimum bound for materials needed for a particular energy output.

Energy obtained from a given reaction is determined from the amount that is reacted and also the reaction itself. The energy, expressed as Wh can be divided into two terms, Volt (V) and ampere-hour (Ah), i.e. Wh = V x Ah. The concept of Ah is fairly straightforward and follows from Faraday's Law of electrolysis (any physical chemistry text book). This law states that 96487 coulombs or 26.8 Ah is released or required for electrochemical reaction of one gram equivalent of a material. For example, 9 g of Al or 6.9 g of Li will produce 26.8 Ah. The voltage concept is slightly more complicated and comes from the relationship of Gibb's free energy and electrochemical potential, EMF.

$\Delta G = nFE$, where ΔG is the change in free energy due to reaction. n is the number of electrons involved in the stoichiometry of the reaction. F is again 26.8 Ah, also known as Faraday. E is the thermodynamic voltage. Therefore, E represents the energy released per gm-equivalent of substance (n = 1). In this context, it is therefore appropriate to cite these voltages and Ah/g of fuel.

From the following table, it can be inferred that the AL-DOS provides the best possible gravimetric energy density from a thermodynamic standpoint and the CFFC provides the best possible volumetric energy density. The advantageous position of lithium is lost as weight and volume of thionyl chloride are considered.

As the name suggests, ALWATT-CFFC is a combination of the ALWATT and CFFC systems; the reaction of the AL-Carrier is a combination of reactions of the ALWATT and CFFC. The ALWATT-CFFC system proposed does not carry hydrogen, but utilizes hydrogen generated from the ALWATT. Since one gram of Al produces 0.11 g of H_2, the total energy that can be obtained from 1 g of Al by the ALWATT-CFFC system is 4.4 + 0.11 x 28.9 = 7.6 Wh. This is the same as in the AL-Carrier system. This is of no surprise.

System	Potential, Volts	Ah/g, Fuel	Wh/g, Fuel	Wh/g, Fuel + Carrier Reactant	Wh/l Fuel + Carrier Reactant
	1	2	3	4	5
Li-$SOCl_2$	3.73	3.9	14.4	1.5	2000
ALWATT	1.47	3.0	4.4	4.4	11800
AL-DOS	2.70	3.0	8.1	8.1	21800
AL-Carrier	2.55	3.0	7.6	7.6	20400
CFFC	1.08	26.8	28.9	28.9	2000*

2.4.2. Losses

The previous section defined the minimum requirements of fuel and oxidizer needed for a given energy requirement. There are inherent losses in a working system when energy is derived from it. These losses are due to:

1) irreversibility
2) chemical imbalance - concentration inequilibria
3) electrical resistances

The losses lead to voltage loss in the system and are often referred to as voltage inefficiency. There is another kind of loss that arises due to unutilized fuel or reactant due to sloughing or parasitic reactions.

The following table shows the thermodynamic and assumed or operating voltages of the above systems and also the stoichiometric Ah/g versus what is to be expected in real situations.

Thermodynamic Vs. Actual or Projected								
System	Voltage			Volt. Eff.	Ampere hr/g of fuel			Utilization Efficiency
	Thermo	Actual	Projected		Thermo	Actual	Projected	
Li-$SOCl_2$	3.73	3.4	-	91	3.9	not known		-
ALWATT	1.47	0.45	-	31	3	2.4	-	0.8
AL-DOS	2.7	-	1.0	37	3	2.4	-	0.8
AL-Carrier	2.55	-	1.2	47	3	2.4	-	0.8
CFFC	1.08	-	0.6	56	26.8	-	18.8	0.7
H_2-O_2 Fuel Cell	1.23	0.9	-	73	26.8	-	-	0.7

* Density of cryogenic hydrogen is 0.07 g/cc

2.4.3 Other Components

Aside from the reactants, a power source needs other components and materials to build a practical working system. These components and materials are discussed further as we discuss each individual system.

2.4.4 Li-$SOCl_2$ System

In this system, aside from the theoretical amount of lithium and thionyl chloride, it has been reported that they need extra thionyl chloride to dissolve the products (sulfur dioxide and the sulfur and lithium chloride). The other materials needed to build a cell are a) separator, b) carbon as cathode and c) current collection. SO_2 that is produced in the cell when discharged dissolves in $SOCl_2$ but exerts a considerable amount of pressure. The cell container needs to be sufficiently strong and thick to withstand the pressure. When all these materials are included, a Li-$SOCl_2$ battery to be used on land has a volumetric energy density of 1000 Wh/l and 500 Wh/Kg (minuteman silo, reported by Altus Corporation, MIT Sea Grant Symposium, November 1988, Massachusetts). Underwater, these values are further reduced to 430 Wh/l[1] and 330 Wh/kg[1]. The exact breakdown of these excess components are not known to Aquanautics.

[1]Private Communication, A Ellanthorpe, DARPA, September 1989

2.4.5 AL-DOS (Aluminum Dissolved Oxygen)

$$2Al + 3/2\ O_2 + 3H_2O \rightarrow 2Al(OH)_3,$$

ΔG° = -372 kcal
E° = 2.7V

Thermodynamic energy density of Al for this reaction = 8.1 Wh/g or 21.8 Wh/ml

Design for 10W, 5 year System (438 kWhr.)		
	kg	l
Thermodynamic Requirement of Al	54	20
* Voltage Efficiency = 37%		
Materials utilization efficiency = 80%		
Actual requirement without pumping	182	68
* Pumping Seawater (30% of gross)		
Actual requirement with pumping	260	97
* Current Density (176 mA/cm^2) gives Al thickness of 1.25 cm.		
* Inter-electrode gap 0.25 cm or 20% of Al		
Gap		19
Sub-total	260	116
* Cell packaging and counter electrode 20% by volume and 1.5 density	34	23
Sub-total	294	139
* Seawater pump	10	5
* System package	-	5
Total	304	149

W-hr/l 2940
W-hr/kg 1440

* Estimate or assumption

2.4.6 AL-Carrier (Aluminum Carrier Battery)

$$2Al + 3/2(L\text{-}Co)_2\text{-}O_2 + 3H_2O \rightarrow 2Al(OH)_3 + 3L\text{-}Co$$

ΔG° = -352 kcal
E° = 2.55V

Thermodynamic energy density of Al for this reaction = 7.65 Wh/g or 20.6 Wh/ml

Design for 10W, 5 year System (438 kWhr.)		
	kg	l
Thermodynamic Requirement	57	21
* Voltage Efficiency = 47%		
Materials utilization efficiency = 80%		
Actual requirement without pumping	152	56
* Pumping Seawater (10%)		
Extra amount required for pumping	16	16
Total requirement	168	62
* Current density 1 mA/cm^2, Al thickness 6.5 cm interelectrode gap 0.5 cm (7.7% of Al)		5
Sub-total	168	67
Cell packaging 20% of volume with density of 1.5	20	13
* Gill	2	3
* Carrier Pump	4	2
* Seawater Pump	6	3
System Packaging	-	8
Total	200	96

Wh/kg	2200
Wh/l	4600

* Estimate or assumption

2.4.7 ALWATT (Aluminum Seawater Battery)

$$2Al + 6H_2O \rightarrow 2Al(OH)_3 + 3H_2,$$

ΔG° = -203 kcal

E° = 1.471V

Thermodynamic energy density of Al = 4.4 Wh/g or 11.8 Wh/ml

Design for 10W, 5 year System (438 kWhr.)		
	kg	l
Thermodynamic Requirement	99	37
Voltage Efficiency = 29%		
Materials utilization efficiency = 80%		
Actual amount needed	426	159
* Extra volume due to shunt protection and packaging (5% of Al by weight, 20% by volume)	23	31
Total	449	190

Wh/kg	975
Wh/l	2300

* Estimate or assumption.

2.4.8 ALWATT-CFFC

			Voltage Eff.	Utilization Eff.
$2Al + 6H_2O \rightarrow 2Al(OH)_3 + 3H_2$	E° =	1.471	29%	80%
$3H_2 + 3/2(L\text{-}Co)_2 \cdot O_2 \rightarrow 3H_2O + 3L \cdot Co$	E° =	1.08	56%	70%

From 1 g of Al, the following energy is derived for this system:

1.471 x 0.29 x 0.8 x 2.98 Wh/g + 1.08 x 0.56 x 0.7 x 2.98 Wh/g
= 2.26 Wh/g (considering the two efficiencies)

With efficiencies as 100%, the energy derived would be (1.471 + 1.08) x 2.98 Wh/g
= 7.64 Wh/g

Design for 10W, 5 year System (438 kWhr.)		
	kg	l
Thermodynamic Requirement	57	21
Actual requirement	192	71
Add 10% for pumping	19	7
Sub-total	211	78
Alwatt needed for packaging & shunt protection	11	16
	222	94
* Fuel Cell	3	2
* Gill	2	3
* Seawater pump	6	3
* Carrier pump	4	2
* System package		10
	230	115

Wh/kg	1900
Wh/l	3800

* Estimate or assumption

2.5 Comparison of Weights and Volumes for a 10W, 5 year System

Figures 2.7 and 2.8 show the breakdown of volume and weight for the five systems discussed here.

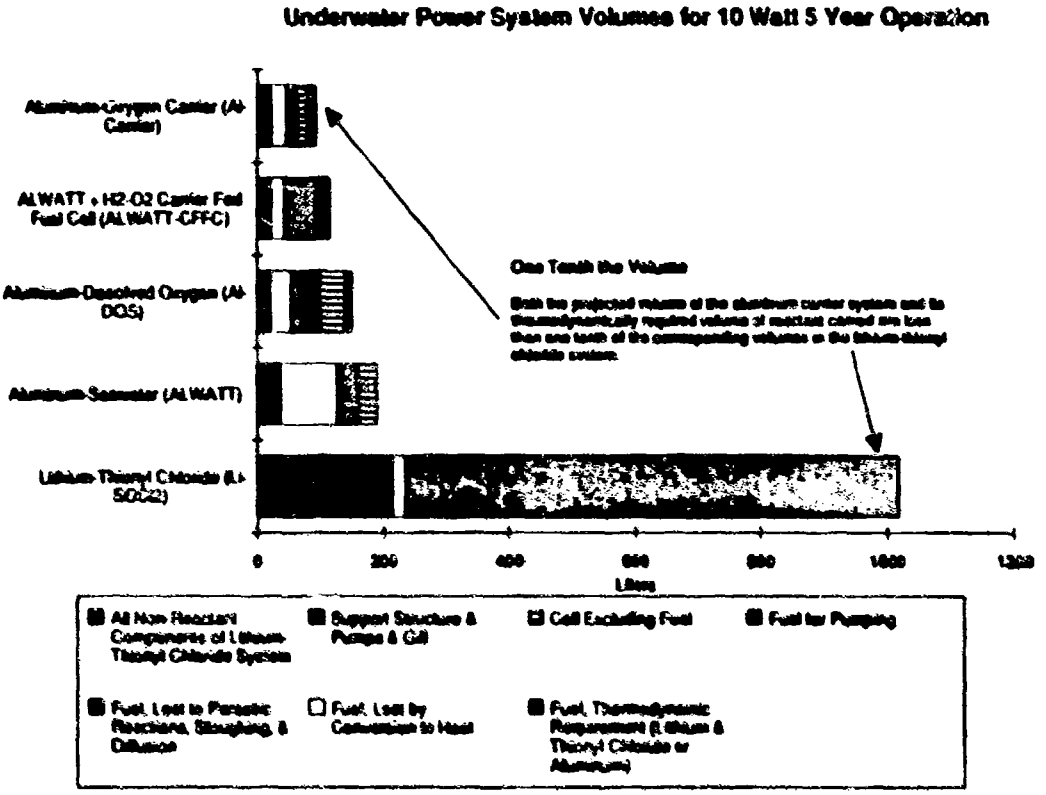

Figure 2.7

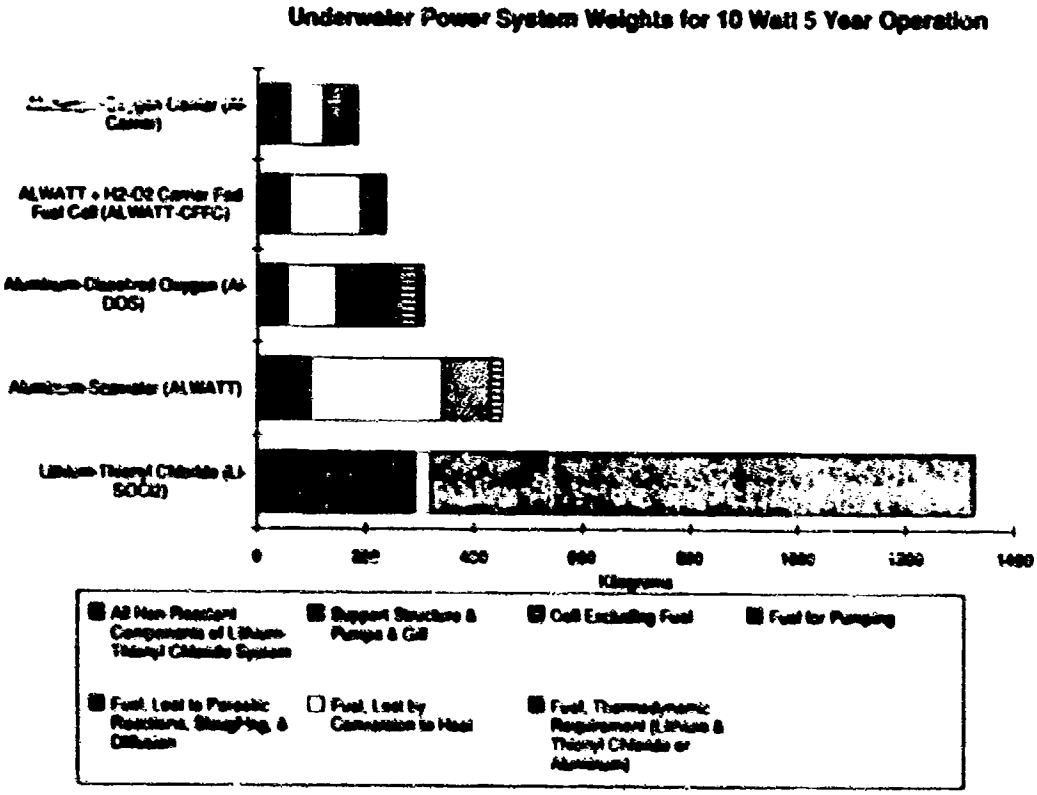
Underwater Power System Weights for 10 Watt 5 Year Operation
ALWATT + H2-O2 Carrier Fed Fuel Cell (ALWATT-CFFC)
Aluminum-Dissolved Oxygen (Al-DOS)
Aluminum-Seawater (ALWATT)
0
400
800
1200
1600
Kilograms
All Non Reactant Components of Lithium-Thionyl Chloride System
Support Structure & Pumps & Gill
Cell Excluding Fuel
Fuel for Pumping
Fuel, Lost to Parasitic Reactions, Straggling, & Diffusion
Fuel, Lost by Conversion to Heat
Fuel, Thermodynamic Requirement (Lithium & Thionyl Chloride or Aluminum)

Figure 2.8

3. WORK TOWARDS CARRIER FEED FUEL CELL

During this quarter the objectives of the research work on the carrier fed fuel cell were primarily to improve the overall cell voltage with a final goal of 0.6 volts. The focus of the effort to improve the cell voltage was on improving anode and cathode performance and reducing ohmic losses. Experiments were carried out with four different types of membrane and electrode assemblies to improve the anode performance and to reduce the ohmic losses through the membrane electrode interface. While almost all experiments used the 23 Suzy P carrier at pH 7, one experiment was performed with 22 Suzy P carrier and the pH varied from 7 to 4. Improvement in the cathode performance resulted from the use of a catalyzed felt.

Membrane and Electrode Assemblies

The membrane and electrode assemblies from Giner Incorporated which were tested this quarter differed from the previous assemblies from Giner in three respects: the membrane material was changed form RAI to Nafion, the bonding between the membrane and the anodic electrode was improved, and the loading of the platinum catalyst was increased. In addition one membrane and electrode assembly from Electrochem Incorporated was tested.

The new membrane and electrode assemblies from Giner performed quite differently from the assemblies previously obtained from Giner as shown in the following table.

Comparison of performance of Giner Membrane and Electrode Assemblies

Experiment	2AM4	2AM11
Membrane	RAI	Nafion
Electrode Platinum Loading (mg/cm^2)	4	20
Current Density (mA/cm^2)	10	10
Cell Voltage	0.17	0.21
Anode - H_2 Ref.	0.25	0.01
Cathode - H_2 Ref.	0.42	0.22
Ohmic Loss	0.10	0.02

As can be seen there were marked reductions in the anode polarization and in the ohmic losses. We believe that both of these improvements are due primarily to the improved bonding of the membrane to the electrode. Giner has had a great deal of experience with Nafion membranes and relative little with RAI and as a result can fabricate much better assemblies with the former membrane. There is little reason to believe that the difference in performance can be attributed to the membrane type alone so we are contemplating experiments with RAI membrane and electrode assemblies with improved bonding.

Although the anode and ohmic losses were much reduced the cell voltage showed little improvement due to the increase in cathodic losses. We believe that the increase in these losses can in part be attributed to an increase in the pH gradient across the membrane. The pH gradient is in part a function of the membrane which justifies continued experimental work with different membranes.

Experiments were also carried out on Giner membrane and electrode assemblies with 4 mg/cm^2 platinum loading. In these experiments the anode and cell performance were not as good as with the higher platinum loading.

The first of a series of membrane and electrode assemblies from Electrochem was tested this quarter. This assembly using the "standard" Electrochem hydrogen anode achieved cell voltages better than the 4 mg/cm^2 platinum loading Giner electrode though not as good as the 20 mg/cm^2. Other as yet untested membrane and electrode assemblies from Electrochem include higher catalyst loadings and may show better performance.

Carrier and pH Variation

One experiment was done this quarter using the 22 Suzy P carrier. The 23 Suzy P carrier had become the standard for experiments since it has the best performance and life time of any carrier tested thus far. The 22 Suzy P was run again however, because previous titration experiments have shown that this carrier binds oxygen at a lower pH than does 23. It was hoped that reducing the carrier pH would reduce the pH gradient in the cell and increase the cell voltage and although in principle this should work the experiment using this particular combination of cell components and carrier showed only a slight improvement in cell voltage.

Catalyzed Felt

The biggest improvement in cell voltage this quarter came from the use of a felt with a surface catalyst bound to it provided by Alupower. The catalyst facilitates the reduction of oxygen at the cathode and improved the cathode voltage by 0.09 volts to give an initial cell voltage of 0.3 volts. The use of catalyzed felt will be the new experimental standard. Additional catalysts for oxygen reduction are known and will be examined first with cyclic voltammetry and then, if they show promise, in a complete fuel cell.

4. WORK TOWARDS AL-CARRIER BATTERY

This quarter several experiments were done with the aim of establishing the feasibility of building a liquid feed aluminum oxygen battery. Experiments were done using seawater and three different oxygen carriers as catholytes.

Aluminum/Dissolved Oxygen System

The aluminum dissolved oxygen system uses seawater to carry dissolved oxygen to the fuel cell where it is reduced. The concentration of dissolved oxygen in seawater is so low that the seawater must flow at a high rate in order to achieve a reasonable cell current density. Experiments were done this quarter which examined the performance of a seawater fed aluminum fuel cell. Experiments at high flow rates (120 ml/min through a 25 cm^2 cell) showed cell voltages of over one volt at current densities of one to two milliamps per square centimeter. At flow rates of 4 ml/min through the same cell the seawater could not provide enough dissolved oxygen to maintain a positive output voltage at a current density of one mA/cm^2 even when the felt treated with the oxygen catalyst was used.

Aluminum/Carrier Experiments

Oxygen carrier solutions can carry nearly two orders of magnitude more oxygen in the same volume of fluid than can seawater and so should be able to maintain reasonable cell current densities at very low flow rates. Carrier run through exactly the same system as was the seawater in the above discussion produced a cell output in excess of one volt at a carrier flow rate of 4 ml/minute.

One of the concerns about the aluminum carrier cell is that the carrier must withstand a pH as high as 12.5 since the reduction of oxygen creates OH^- ions which flow from the cathode to the anode only due to their concentration gradient. Three ligands were used to make carrier solutions for use in this system: tetren, crude Suzy and 23 Suzy P. The first two of these were examined because they were thought to be more suitable for use at high pH. However the performance of 23 Suzy P, which in the past has proven to be a more stable compound, was found to be comparable to the performance of the others. Experiments were run with the intention of examining the carrier degradation over time. It was found that the experimental cell design was poorly suited to the aluminum seawater anode and the cell voltage declined due to clogging of the anolyte seawater flow path with precipitates and the formation of internal cells between the aluminum and the titanium current collector. The carrier survived three cell rebuilds over a week of nearly continuous operation with only very little degradation in performance before the experiment was abandoned. We plan to redesign the anode side of the cell and repeat these experiments in order to obtain meaningful data about the carrier lifetime in this system.

5. ALWATT BATTERY

The ALWATT battery in the ALWATT-CFFC scheme is not only the source of hydrogen, it also produces power. It was calculated based on the energy densities and hydrogen generation characteristics that about 20-25% of gross power will be generated by the ALWATT battery. Aquanautics recently asked Alupower to model the ALWATT design to minimize the volume needed and maximize the power generated for a given hydrogen requirement. Their report is attached as Appendix 1.

The study shows that the ALWATT cell can be re-designed to obtain 1700 Wh/l and 700 Wh/kg with 50% fuel utilization. Alupower recently informed us that they have recently developed an aluminum alloy with 80% fuel utilization.

As a result of these developments, the ALWATT battery would generate approximately 45% of the gross power and the CFFC would produce the rest. The energy densities for the ALWATT are recalculated on the basis of new utilization efficiency in Section 2.

Note also that the projected ALWATT battery energy density is about four times that of the lithium thionyl chloride battery and is much safer to handle.

6. WORK TOWARDS CARRIER

Summary

EOC experiments using compound 72 showed that lifetime was related to the concentration of free oxygen dissolved in the carrier. The bound oxygen is not responsible for the degradation. Since the free oxygen concentration cannot be higher than that in seawater for the gill, the implication is therefore that underwater operation favors the carrier lifetime.

Voltammetry studies with compound 64 show satisfactory operation with sulfate and fluoride as the counter ions. These ions are more compatible with the anode of the fuel cell. Perchlorate, however, causes polymerization. Static lifetime tests on some tetradentate polyalkylamines have shown lifetimes of greater than two months.

6.1 Experimentals

6.1.1 The EOCs were configured to operate with pure oxygen unloading while two small systems were maintained with air sweep unloading for initial screening purposes. Two parallel experimen. . were carried out using a single batch of compound 72 with MDAMF added as mediator. Both experiments gave >90% pure oxygen at about 160 watts per liter per minute for 12 days. Both solutions failed as judged by the electron count values at fourteen days (pH=7). These results confirm a previous experiment with Compound 72 which was run in the pure oxygen unload mode. The EOC was reconstructed to minimize the volume of carrier in the unloading section between the anode outlet and the cathode inlet and another batch of compound 72 was prepared. A power increase at thirty-three days occurred despite adjustment of the pH and is thus due to final failure of the carrier. In the previous quarterly report the lifetime of compound 72 was reported to be six weeks while the oxygen is swept from the unloader by an airstream. The trend is thus unmistakable that the longer the released oxygen is allowed to remain in contact with the carrier the more rapid is the degradation. Now the binding constant of compound 72 is such that the carrier should be fully saturated with oxygen under air. Thus, if the bound oxygen is responsible for the degradation, why should there be a dependence upon the carrier contact time with high purity oxygen? The implication is therefore clear that a second oxygen molecule which is free in solution is responsible for the degradation.

In the power systems under consideration, no release of oxygen is envisioned. Thus the free oxygen concentration in the carrier will not exceed that in seawater. If the irreversible reaction of carrier with oxygen depends on the concentration of free oxygen then the fuel cell system creates a favorable situation for the carrier lifetime.

6.1.2 Cyclic voltammetry of compound 64 was carried out using perchlorate, fluoride and sulfate as the counter ion. Both fluoride and sulfate gave satisfactory results. Indeed the use of sulfate gave clear evidence in the voltammetry of the release of Co(III). The use of perchlorate presented no difficulties while oxygen was excluded and a normal voltammetric response was observed. As soon as oxygen was introduced, however, a brown precipitate formed immediately and the electrode was passivated.

6.1.3 Static lifetime tests were carried out on compounds 244, 245 and 246. Each solution was prepared as a 0.5 mM solution and thoroughly saturated with air by an airstream. The UV/visible spectrum was then recorded at intervals until the charge transfer band no longer decreased with time. Each solution was stored in a graduated flask open to the air and was vigorously shaken before each measurement. There are two parts to the process. The first part is clearly mass transport controlled by the availability of oxygen

while the second part corresponds to an adequate supply of oxygen since the concentration of carrier has declined below the level where it can consume all of the available oxygen. The implication once again is that a second oxygen molecule is responsible for the degradation.

6.2 Workplan for Next Quarter

6.2.1 Test low pH unload concept. Examine several carriers for acid-base behavior. Eliminate carriers which react slowly to the addition of acid to the solution. Obtain electrodes coated with Nafion and bonded to a Nafion membrane with a hydrogen anode bonded to the other side. Test these electrodes with the carriers which rapidly release oxygen with addition of acid. Test uncatalyzed and catalyzed Nafion coated electrodes.

6.3.2 Develop quantitative methods using Rotating Ring Disk Electrode Voltammetry (RRDEV) to examine carrier behavior at the electrode. Use the methods to study at least five different families of carrier and correlate the observed behavior with tests in the fuel cell rigs. The behavior will be studied as a function of pH (low pH for CFFC and high pH for AL-Carrier). Choose best carrier families for each application.

6.3.3 Develop lifetime testing for carrier screening. This involves static-lifetime EOC testing and fuel cell testing in conjunction with RRDEV data from 6.3.2.

7. GILL

7.1 Introduction

This report describes testing performed on a rectangular gill cartridge fabricated for Aquanautics by Applied Membrane Technology (AMT) of Minnetonka MN. Details of the gill cartridge fabrication are presented in a report submitted by AMT which is attached as Appendix 2. The gill cartridge was intended to test the viability of using a membrane loader to transfer oxygen from seawater to carrier in an underwater power source employing Aquanautics' proprietary oxygen carrier technology. The gill cartridge was fabricated according to specifications that were defined at Aquanautics after a gill power-volume model had been developed and studied. Results of the gill power-volume relationship are included in the Quarterly Report for the quarter spanning the months of April to June 1989.

Testing of the gill membranes was performed during the period of September 3 to September 15, 1989. Most of the testing was preliminary and intended to verify the gill power-volume model. This report shall, therefore, include not only the results of the gill testing, but shall also include a comparison of the experimental results with the predictions of the model.

7.2 Background

The work described in this report was performed as part of the DARPA contract to investigate the use of Aquanautics' proprietary oxygen carriers in producing power undersea. In the systems being investigated the oxygen dissolved in seawater is extracted by the carrier, transported to a fuel cell and consumed in a reaction with a fuel producing electrical energy. The fuel can either be hydrogen produced by an aluminum corrosion cell or aluminum itself. In both cases the carrier containing bound oxygen is fed directly to the cathode of the fuel cell where the bound oxygen is reduced. The gill is the location at which the oxygen transport from seawater to carrier takes place.

A major parasitic loss in the system described in the preceding paragraph is attributable to the power required to pump seawater through the gill. The pumping power for seawater flow through the gill is a function of the gill size and configuration as well as the flux of oxygen required to produce the specified output power. The model derived to analyze the gill consisted of two equations, one describing the power as a function of the gill volume and the second expressing oxygen flux as a function of gill volume. These equations are amenable to use for optimizing the gill volume as described in the Quarterly Report for the period April-June 1989.

The gill configuration chosen for this purpose consists of a rectangular bed of hollow fibers where the carrier flows inside the fiber lumen and seawater across the outside of the fibers in a direction perpendicular to the plane of the fiber bed. This configuration has been shown to offer maximum mass transport with minimal losses due to drag[2]. Accordingly, AMT was requested to fabricate eight cartridges for testing at Aquanautics. Four of these cartridges were to be constructed of microporous hollow fiber membranes, while the other four membranes were to be constructed of microporous fibers coated with AMT's proprietary oxygen permeable solid layer. Each type of membrane cartridge was to be constructed in two configurations, one with an inter-fiber spacing factor of 2.5 and the

[2]Yang, M.C., and Cussler, E.L., "Designing Hollow-Fiber Contactors," *AIChE J.*, 32, 11 (1986)

other configuration involving a factor of 1.5. The inter-fiber spacing factor refers to the ratio of the center-to-center distance between the fibers to the outer diameter of the fibers. The testing reported on here involves cartridges that were made from plain microporous hollow fibers with an inter-fiber spacing factor of 2.5.

7.3 Experimental Setup

Figure 7.1 shows the schematic of the experimental setup used for testing oxygen flux through the gill cartridges. The gill cartridge consisting of a rectangular fiber bed made from microporous hollow fiber membrane was housed in a flow box which had an entry port and an exit port on either side of gill. Figure 7.2 depicts the design of the flow box used for the gill cartridge. The flow box was connected to a pump which pumped artificial seawater from a tank equipped with a chiller and an aerator to maintain temperature and the oxygen content of the seawater respectively. The gill cartridge was swept with nitrogen gas on the inside of the fiber lumen in these preliminary experiments. It is expected that carrier will be used in later experiments.

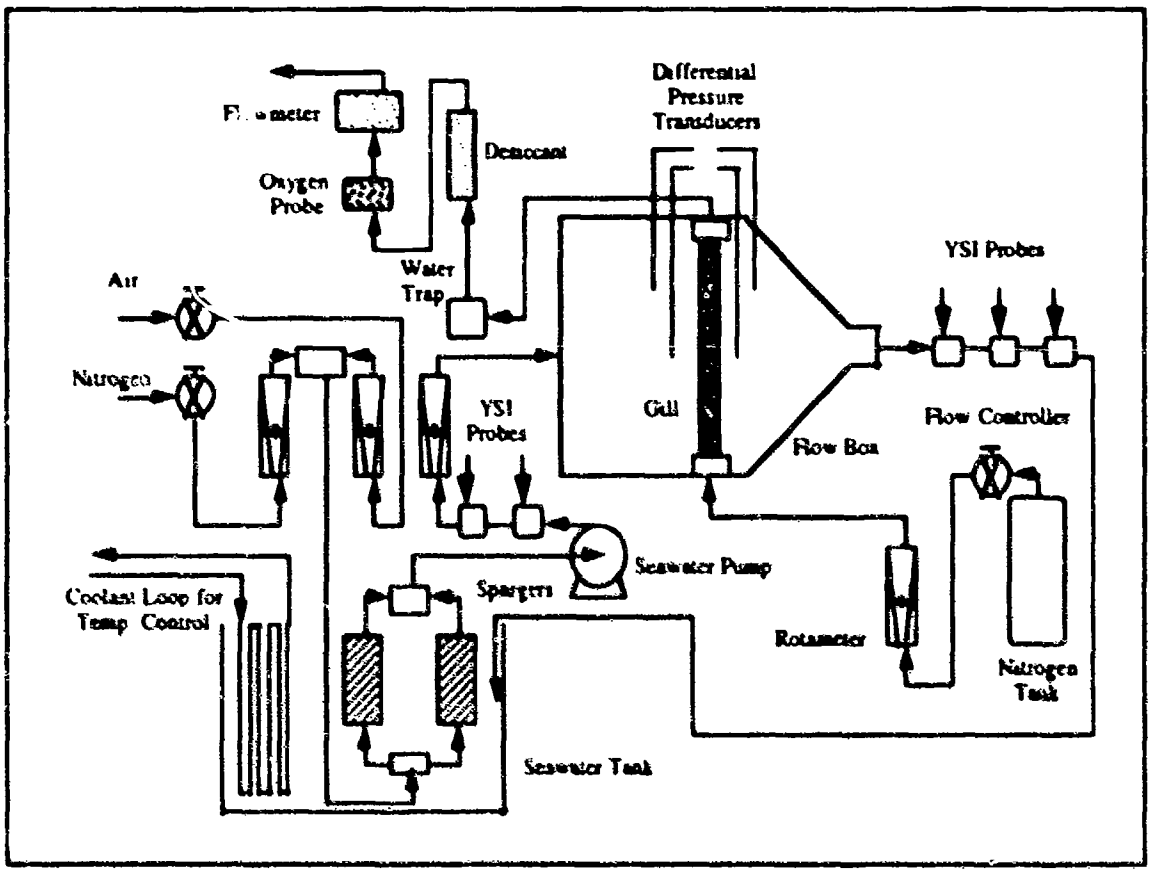

Figure 7.1 Schematic of Experimental Setup.

The oxygen content of the seawater entering the flow box and leaving it was measured using Clarke-type probes manufactured by Yellow Springs Instruments (YSI). Two probes were used before the gill and three after the gill to ensure redundancy in case of probe failure. The flow rate of seawater was measured using a rotameter with a range of 0-4 gpm. Flow rate of seawater could be varied by using a system of valves with a bypass

arrangement or by adjusting the speed of the pump. Nitrogen from a pressurized tank was fed to a flow controller through a pressure regulator and then to the gill cartridge through a rotameter. The rotameter was used only to set the flow rate of the nitrogen. The oxygen-enriched sweep gas exiting the gill cartridge was passed through a Teledyne probe and a hot wire anemometer to measure the oxygen content and the flow rate respectively. The seawater pressure drop across the gill cartridge was measured using differential pressure sensors from Omega Instruments. The pressure difference was measured at two points, namely at half and quarter height of the gill as shown in Figure 7.2.

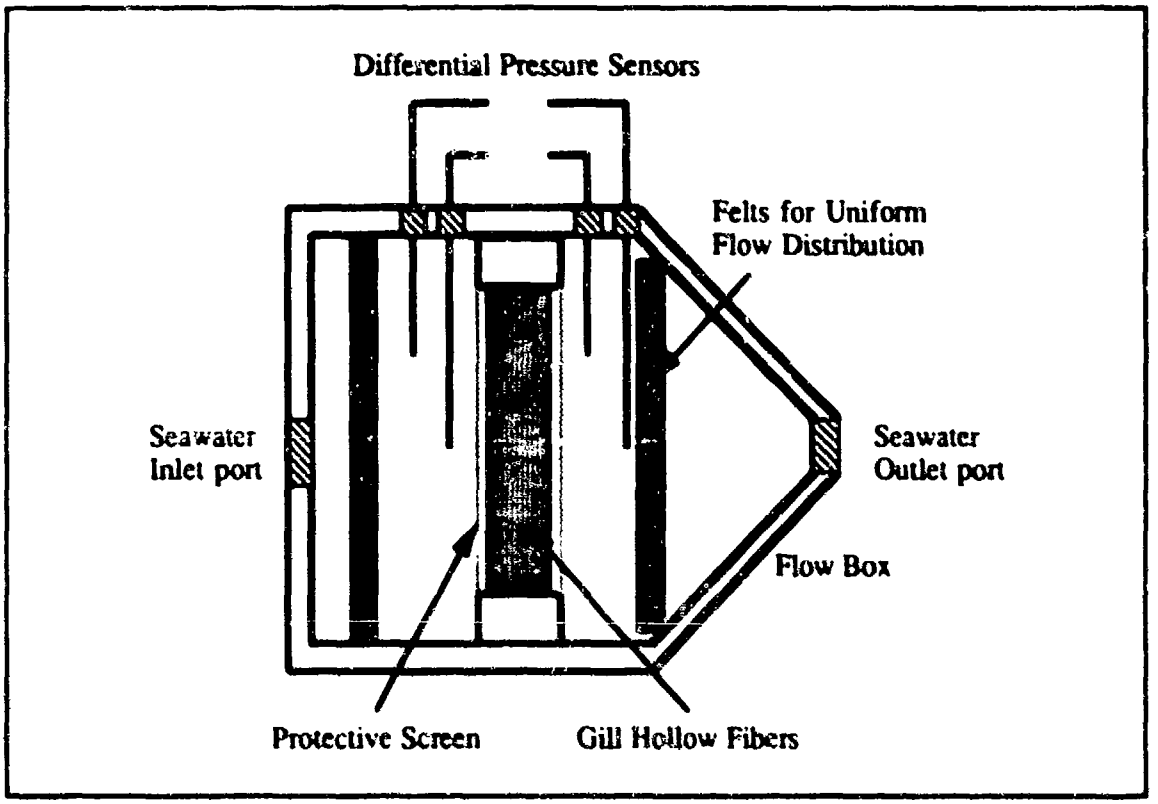

Figure 7.2 Design of Flow Box for Gill Cartridge Testing.

Data from the YSI probes were acquired using an eight-channel data acquisition system connected to an IBM XT computer, while another system was dedicated to the nitrogen sweep gas measurements and the pressure drop data.

7.4 Procedure

The experimental system depicted in Figure 7.1 was assembled and seawater flow from the seawater tank started. The seawater tank was sparged with either air or the appropriate mixture of air and nitrogen to simulate 100% saturated and unsaturated seawater respectively. The nitrogen flow was turned on and set at 500 ml/min using the rotameter and flow controller. Data acquisition was started with the seawater flow set at the lowest value and data taken until approximately 15 minutes of steady state operation was realized. Data points were recorded every three minutes and therefore data was acquired until five

consecutive data points showed less than 10% deviation. The seawater flow rate was then stepped up to its next higher value and the experiment repeated.

Three sets of experiments were performed, with seawater conditions being the only parameter that was changed. The seawater conditions for the three sets of experiments were as follows:

1) Temperature = 3 C; Initial Oxygen concentration = 6.8 ml/l,
2) Temperature = 8 C; Initial Oxygen concentration = 1 ml/l, and
3) Temperature = 8 C; Initial Oxygen concentration = 5.8 ml/l.

The first and last experiments were performed with air saturated seawater and the Oxygen concentration values shown above correspond to saturation at the respective temperatures. In the second experiment, a mixture with a 1:6 volume ratio of air to nitrogen was sparged through the seawater tank to achieve the 1 ml/l concentration.

The nitrogen flow rate was not expected to affect the mass transport of oxygen since the boundary layer on the seawater side controls the flux rate. This was checked by running the nitrogen at 800 ml/min for a couple of data points and comparing the oxygen flux with that realized at a nitrogen flow of 500 ml/min, all other conditions remaining constant. No difference was seen and the experiments were all performed with the nitrogen flow rate set at 500 ml/min.

Prior to each experiment, the YSI probes were calibrated using a two point calibration method. The seawater was saturated with air at the operating conditions and the gain on the signal amplifier adjusted so that the output from the amplifier for each of the probes was 1 V. The seawater was then sparged with nitrogen to get a "dark current" reading on the different probes. The actual experiment was conducted only after the YSI probes were thus calibrated. The gill remained inactive during the calibration to ensure that the probes upstream and downstream of the gill flow box were subject to the same seawater oxygen concentrations.

7.5 Results

The results of the various experiments are presented in the form of two types of plots. The first plot graphs oxygen flux as a function of the seawater flow rate, while the second plots seawater pumping power as a function of seawater flow rate. Plots were worked out for all three experiments and are presented as Figures 7.3 through 7.8. Data analysis was done using the Excel spreadsheet program on an IBM compatible computer and transported to a Macintosh for presentation.

The seawater flow rates were obtained from the rotameter that was placed in the seawater loop prior to the flow box. The oxygen flux was calculated using two methods. The first entailed using data from the YSI probes to calculate the oxygen content of the water entering and leaving the gill flow box. The oxygen content of the seawater at any probe was calculated by using the expression,

$$C_i = \frac{E_i - E_d}{E_a - E_d} S_o \qquad (7.1)$$

where, C_i is the concentration of dissolved oxygen in seawater at the probe i (standard ml/l),
E_i is the reading of probe i (V),
E_d is the "dark current" reading of probe i obtained during calibration (V),
E_a is the reading of the probe i in air saturated seawater (V), and
S_o is the solubility of oxygen in seawater at the operating temperature (standard ml/l).

The oxygen concentrations calculated from probe readings before and after the flow box were averaged and the oxygen flux across the membrane calculated using the expression shown in Equation 7.2.

$$N = (C_{si} - C_{so})\ Q \tag{7.2}$$

where, C_{si} is the oxygen concentration of seawater entering the flow box (standard ml/l),
C_{so} is the oxygen concentration of seawater leaving the flow box (standard ml/l),
Q is the flow rate of seawater through the gill box (l/s), and
N is the oxygen flux rate (standard ml/s).

The oxygen flux was also calculated from measurements made at the nitrogen sweep outlet. The value of the oxygen flux from the nitrogen sweep side was calculated using the expression given in Equation 7.3.

$$N = Q_s\ p_o \tag{7.3}$$

where, Q_s is the flow rate of the sweep gas (standard ml/s),
p_o is the partial pressure of oxygen in the exiting sweep gas (atm), and
N is the oxygen flux rate (standard ml/s).

The flow rate of the sweep gas was measured using a gas flowmeter from Omega Instruments that is based on the hot wire anemometer principle, while the oxygen content of the sweep gas was measured by a Teledyne oxygen probe.

The pressure drop across the gill cartridge was measured at two points using differential pressure transducers. The readings were averaged and the power to pump seawater calculated from this average value using Equation 7.4.

$$P = \Delta p\ Q \tag{7.4}$$

where, P is the power to pump seawater (W),
Δp is the pressure drop across the gill cartridge (N/m^2), and
Q is the seawater flow rate (m^3/s).

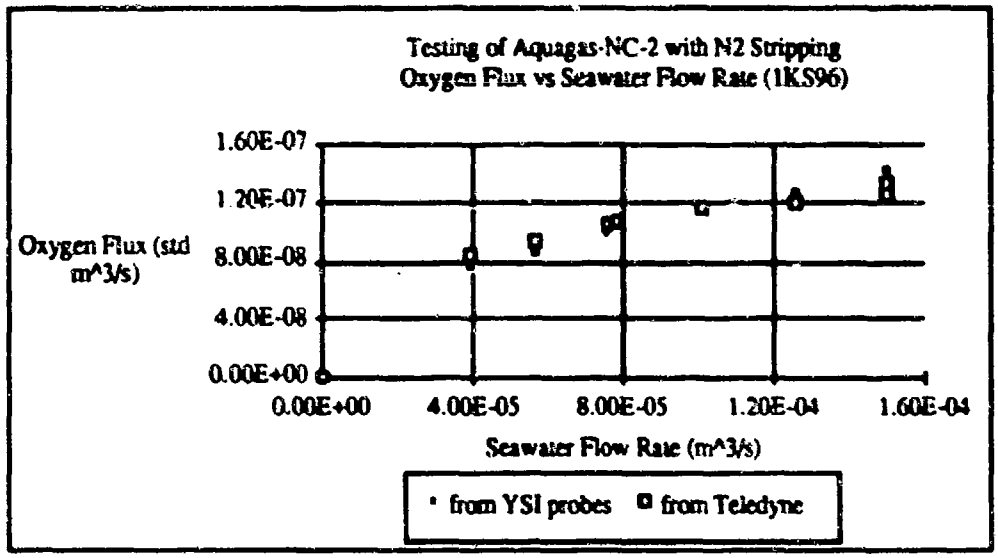

Figure 7.3 Oxygen Flux vs Seawater Flow Rate in 1KS96.

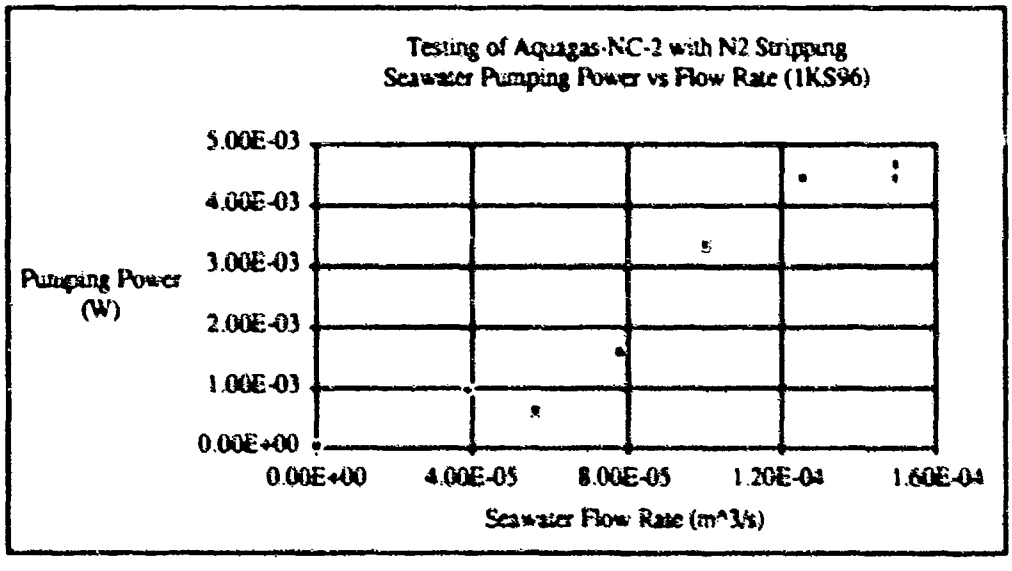

Figure 7.4 Seawater Pumping Power vs Seawater Flow Rate in 1KS96.

Figures 7.3 and 7.4 refer to the first experiment listed in the preceding section (1KS96). Figures 7.5 and 7.6 are for the second experiment (1KS98), and Figures 7.7 and 7.8 are for the last experiment (2KS02).

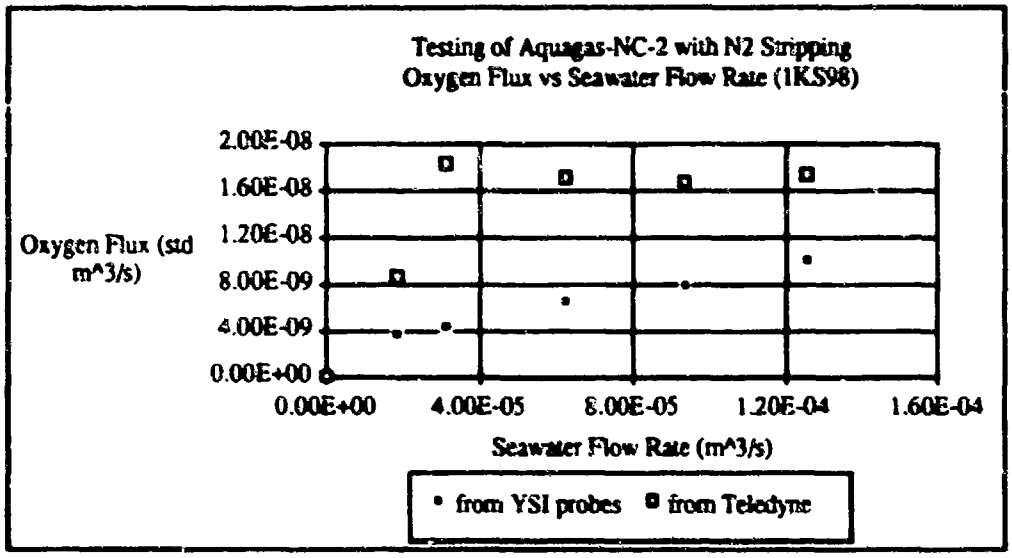

Figure 7.5 Oxygen Flux vs Seawater Flow Rate in 1KS98.

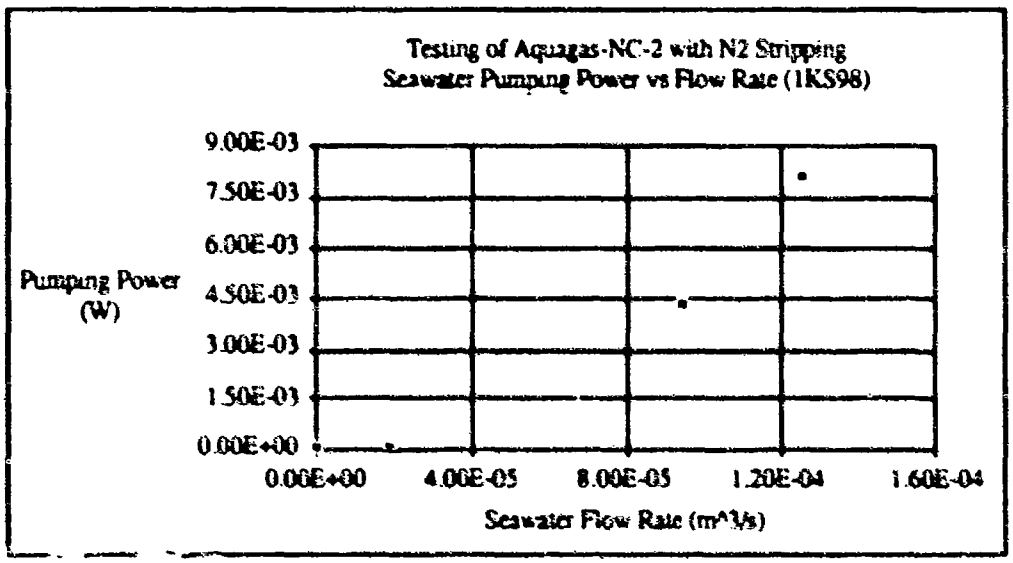

Figure 7.6 Seawater Pumping Power vs Seawater Flow Rate in 1KS98.

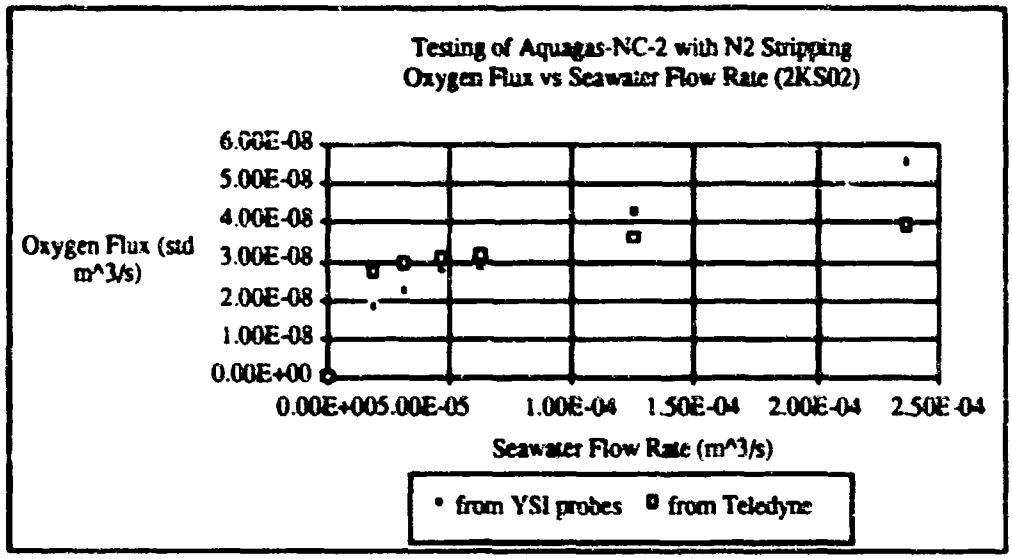

Figure 7.7 Oxygen Flux vs Seawater Flow Rate in 2KS02.

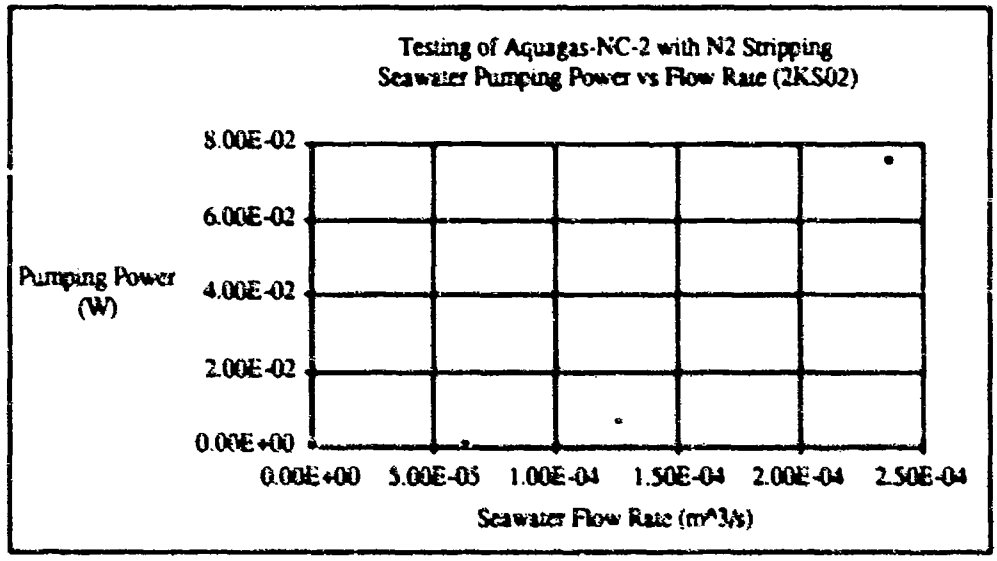

Figure 7.8 Seawater Pumping Power vs Seawater Flow Rate in 2KS02.

7.6 Discussion

7.6.1 Oxygen Flux

The maximum oxygen flux was seen in the experiment designated 1KS96. Oxygen flux rates of 8.5 ml/min were noticed in this experiment. It is also obvious from Figure 7.3 that the system mass balance was well established in this experiment, i.e., the oxygen flux shown by the Teledyne probe matches that calculated from YSI probe readings. This

agreement extends to all seawater flow rates investigated. The seawater temperature in this experiment was 3 C and the oxygen concentration under conditions of air saturation was calculated to be 6.8 standard ml/l for seawater.

The second experiment, namely 1KS98, was conducted with seawater at 8 C and the oxygen concentration at about 1 standard ml/l. The oxygen flux noticed from this experiment proved to be much smaller than those obtained in 1KS96 as is obvious from Figure 7.5. In this instance there was no agreement between oxygen flux values calculated from the seawater and nitrogen loops. The Teledyne probes showed that the oxygen flux rate reached an asymptotic maximum at a seawater flow rate of 2 l/min. The YSI probes, however showed that the oxygen flux increased gradually as the flow rates were increased. The Teledyne probes showed a maximum flux of about 1 standard ml/min, while the YSI probes showed a flux of approximately 0.6 standard ml/min at the maximum seawater flow rate.

The last experiment, namely 2KS02 was conducted with an oxygen concentration of about 5.8 standard ml/l and a seawater temperature of about 8 C. The agreement between oxygen flux values calculated from the Teledyne probe and the YSI probes was found to be better than in the case of 1KS98. The YSI probes, however, showed larger fluxes at higher seawater flow rates while the converse was true at the lower values of the seawater flow rate. A maximum flux of 3.3 standard ml/min was measured by the YSI probes, while the Teledyne probes yielded a maximum flux of 2.4 standard ml/min.

The difference between the YSI probe and Teledyne probe readings in 1KS98 could be attributed to lack of resolution of the Teledyne probes. The high nitrogen sweep rates meant that the oxygen content of the exiting sweep was very low and this was especially true in the case of the low seawater oxygen concentrations. This meant that the Teledyne probes were always operating at the low end of their range and were therefore subject to errors.

The second point of importance is the seeming degradation of membrane performance between 1KS96 and 2KS02. Even allowing for the slightly lower oxygen concentration in the latter experiment, the degradation in oxygen flux cannot be explained. The higher temperature in 2KS02 should help the oxygen flux because of the higher oxygen diffusivity associated with higher temperatures.

7.6.2 Seawater Pumping Power

The seawater pumping power in the first two experiments (Figures 7.4 and 7.6) was measured to be in the milliwatt range. The pressure drop across the membrane cartridge was found to be very low and of the order of hundreds of Pascals (N/m^2). The power was seen to increase as a function of the seawater flow rate, though the data was not considered reliable due to inaccuracies in the differential pressure sensor. The sensors used in this experiment had a range of 5 psi (34,000 N/m^2) and were therefore operating in the bottom 1% of their range. The readings from the transducers were not considered reliable for this reason. In the last experiment (2KS02; refer to Figure 7.8) the seawater flow rate was increased sufficiently for the pumping power to exceed 75 milliwatts. The results from 2KS02 show that the power does not increase linearly with flow rate but that it is a higher order polynomial function of the flow rate, as expected.

7.6.3 Comparison With Model Predictions

The data acquired from 1KS96 is compared with the predictions of the gill power-volume model in Figures 7.9 and 7.10. In Figure 7.9 the measured oxygen flux is compared with the predictions of the model, while Figure 7.10 compares the seawater pumping power measured with the simulated values.

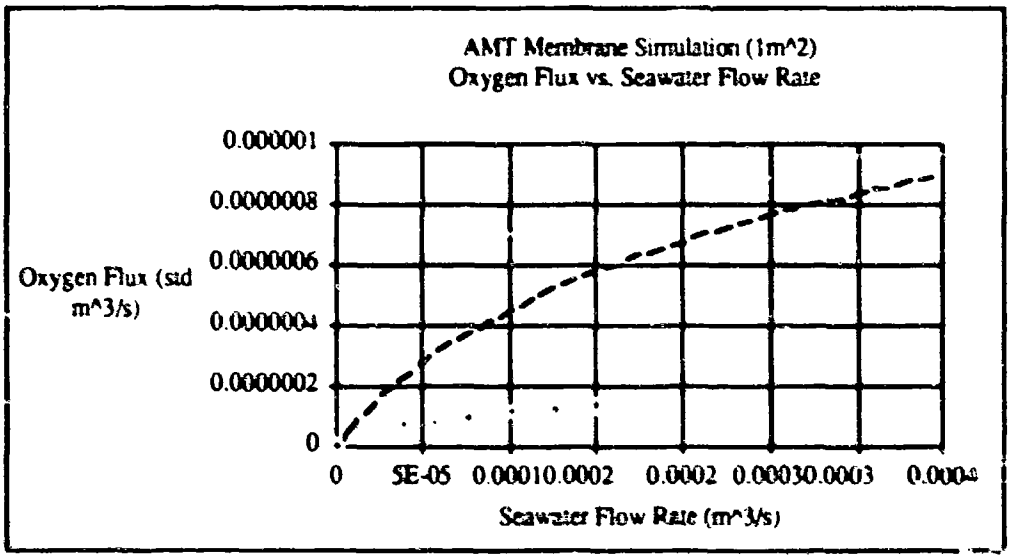

Figure 7.9 Comparison of Measured Oxygen Flux with Predictions.

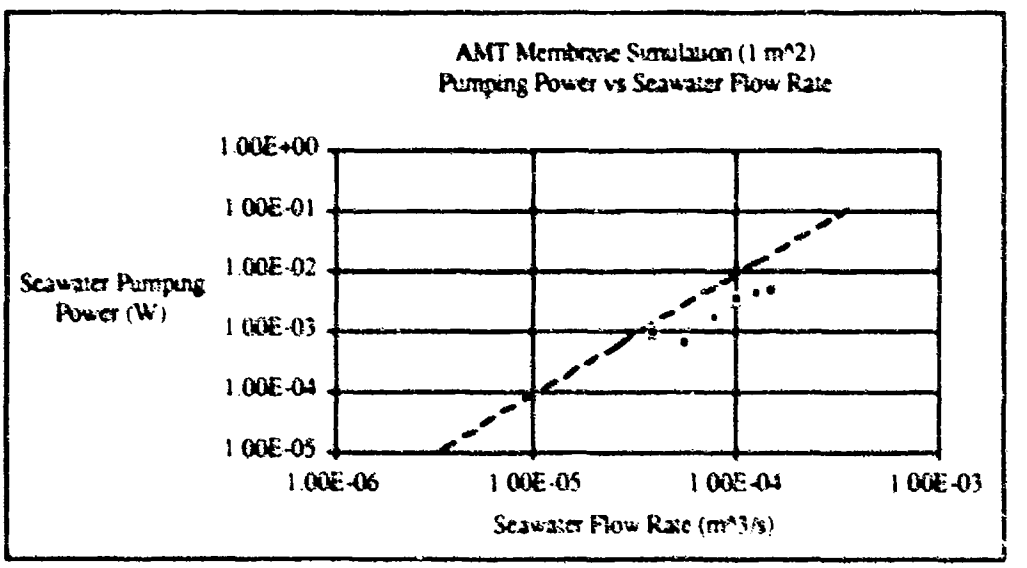

Figure 7.10 Comparison of Measured Seawater Pumping Power with Predictions.

The predicted values were obtained by using the equations for pumping power and oxygen flux that have been developed for rectangular fiber beds. These equations are shown below and details of their derivation are available from the quarterly report for April-June 1989. The equations[3] derived in that report were modified for the gill fiber weaving configuration, which in the case of the cartridges tested here was unidirectional.

$$\frac{P\,V^2}{Q^3\,l^2\,\rho} = 13.5093\,\frac{\xi^2}{(\xi-1)^{1.6}}\left[\frac{\upsilon}{D}\right]\left[\frac{V\,D}{Q\,l^2}\right]^{0.2}\left[\ln\frac{C_{si}}{C_{si}-N/Q}\right]^{1.2} \qquad (7.5)$$

$$\left[\ln\frac{C_{si}}{C_{si}-N/Q}\right] = 4.3354\left[\frac{D^2\,V^2\,l}{\xi^5\,(\xi-1)\,d_o^5\,Q^2}\right]^{1/3} \qquad (7.6)$$

The values of the terms P (pumping power) and N (oxygen flux) were obtained by solving equations 7.5 and 7.6 respectively and were plotted as a function of Q (seawater flow rate) for the cartridge which was tested.

It can be seen from Figure 7.9 that the oxygen flux obtained in the experiment was well below the value predicted by the model. The power, however was also lower than that predicted as shown in Figure 7.10 leading to the possibility that the flux could be improved by increasing the flow rate and expending more power on the pumping.

7.6.4 Problems Encountered in Experiments

The experiments conducted had two sources of problems. These were,

1) Insufficient pumping capacity, and
2) Leaking cartridges.

The pump available for the experiment could only discharge up to 4 gpm of seawater into the experimental setup and therefore flux data could not be acquired at flow rates sufficiently large to cause expenditure of measurable quantities of pumping power. Therefore all measurements were made at the lower end of the pumping power spectrum. A larger pump capable of greater discharge is necessary to investigate fluxes at higher flow rates. At the highest flow rate, namely 4 gpm the velocity of seawater through the gill was only 2.8 cm/s and higher flow rates will be necessary to achieve higher flux rates.
The second problem, namely leaks in the cartridge could have led to a further impedance to oxygen flux across the membrane. Water collecting inside the fiber lumen can block off a lot of individual fibers causing all nitrogen sweep to flow through only a fraction of the fibers. This decreases the area of the membrane available for mass transport and could have affected the flux. Moreover the liquid on the inside of the fibers can form a relatively oxygen-impermeable layer causing lowered flux rates.

7.7 Conclusions

The following conclusions were drawn from the gill testing work described here:

1) The oxygen flux from seawater to the nitrogen sweep is a function of the seawater flow rate. The flux values noticed in the first experiment (1KS96)

[3] Aquanautics Document, "Fourth Quarter (FY 1989) Technical Report," Section 2 (1989)

were not obtained again when similar conditions were used again (2KS02). The oxygen flux values seen in the experiment with low initial oxygen concentrations (1KS98) were disappointing, and could have been affected by the entry of water into the fiber lumen, as well as the inability to pump larger quantities of seawater through the gill.

2) The performance of the membranes could have been affected by the water leaking into the cartridge. The cartridges shall be sent back to their fabricators for repair and tested again after their return.

3) The model over-predicted the oxygen fluxes that were obtained, while the seawater pumping power was less than that predicted by the gill model. The model shall be compared with data obtained from non-leaking gill cartridges for a more complete analysis.

4) The pump attached to the test setup was not powerful enough to produce flow rates in excess of 4 gpm of seawater. A new and more powerful pump shall be arranged to facilitate faster flow rates and investigation of the oxygen flux at higher pumping powers.

5) The gill design goal for the demonstration unit is 3 l of volume for a 42 ml/min flux from a concentration of 1 ml/l with a power consumption of 0.25 W. The best performance obtained with the gill cartridge that was tested was a flux of 8.5 ml from a concentration of 6.8 ml/l with a gill volume of 0.57 l using a pumping power of 0.005 W.

7.3 Work Planned for Next Quarter

The experimental setup shall be fitted with a bigger pump in an effort to increase the seawater flow rate and experiments repeated with all the cartridges that are being fabricated for this project. This shall include the coated cartridges that have been recently delivered as well as the uncoated cartridges after the leaks have been repaired.

In addition to testing, the cartridges that were determined to leak shall be sent back to AMT for repairs and retested upon their return.

Appendix 1

Comparison of Hydrogen Storage/On-Line Generation Methods
and
ALWATT Hydrogen Generator Power Study

Alupower, Inc.

COMPARISON OF HYDROGEN STORAGE/ON-LINE GENERATION METHODS AND ALWATT HYDROGEN GENERATOR POWER STUDY.

Prepared by
Shailesh A. Shah and B.M.L.Rao
Alupower Inc.
6 Claremont Road, Bernardsville, NJ 07924

For
Aquanautics Inc
980 Atlantic Avenue
Suite #101
Alameda, CA 94501

July 26, 1989.

TABLE OF CONTENTS

EXECUTIVE SUMMARY

This report is a study of the following two topics:

(i) Comparison of Hydrogen Storage/on-line Generation Methods (Section-I),

(ii) ALWATT Hydrogen Generator Power Study (section-II).

The first one was to assess the technoeconomics of various methods of hydrogen supply for the Aquanautics underwater SPE fuel cell. The second study was to optimize an ALWATT cell that is capable of providing 25 watts and 696 ml/min of hydrogen for one year for the 100W fuel cell system. The study was carried out as per guidelines from Dr. Sam Mohanta.

SECTION-I: The hydrogen storage/on-line generation options are examined. These include: (i) Compressed gas storage, (ii) Liquid hydrogen storage, (iii) Metal hydrides (iv) Methanol reformer, (v) Aluminum corrosion and (vi) ALWATT cell. Of these, methods (i) to (iv) are capital intensive because of pressure-hull requirement and hence, are not preferred. Other reasons for excluding these include volumtric inefficiency (compressed gas), safety (liquid hydrogen) and additional energy requirements (methanol reformer, $FeTiH_2$). Calcium hydride (CaH_2), aluminum corrosion and ALWATT are on-line generation methods and do not require a pressure-hull because of the open nature of the system. The cost/kg of hydrogen from these methods are of the following order: CaH_2 > ALWATT > Aluminum corrosion Among the last two, ALWATT is preferred because it is the only method that provides hydrogen and supplemental electric power.

SECTION-II: The power study has resulted in the mization of ALWATT cell with respect to volume and weight. The results are presented in the form of 'watts/unit volume' and 'watts/unit weight' that are scalable to Aquanautics power requirements of present and future needs. Maximum power density is sensitive to cell volume. Specifically, an ALWATT cell capable of delivering 25 watts along with 696 ml/minute of hydrogen is modeled. Cells with about 1 cm aluminum anodes and 0.1 cm gap operating at 0.6 mA/cm^2 have maximum volumetric power density. Details of the analysis is presented in section-II. Optimal power and energy densities of ALWATT cell and battery are presented in Table-1.

SECTION -I

COMPARISON OF HYDROGEN STORAGE/ON-LINE GENERATION METHODS

COMPARISON OF HYDROGEN STORAGE/ON-LINE GENERATION METHODS FOR AQUANAUTICS FUEL CELL

Shailesh A. Shah and B.M. L. Rao
Alupower Inc.,
6 Claremont Road, Bernardsville, NJ. 07924, U.S.A

I. INTRODUCTION

Various types of hydrogen/oxygen fuel cells are used in terrestrial and space applications (1). Oxygen is either derived from air or supplied from a cryogenic storage tank. Recently, Aquanautics has developed an artificial gill that concentrates the dissolved oxygen from seawater and has proposed its use in a hydrogen-oxygen fuel cell for underwater application. This article addresses the cost of hydrogen supply for Aquanautics fuel cell.

A number of options exist for the hydrogen supply (2). They are: (i) Compressed gas, (ii) Liquid hydrogen, (iii) Metal hydride, (iv) Methanol reformer, (v) Aluminum corrosion and (vi) ALWATT ™ hydrogen generator. The first three methods provide stored hydrogen and the last three relate to on-line generation of the fuel. Of these, the ALWATT hydrogen generator is new (3). It provides not only the required hydrogen but also generates electricity to supplement the total electrical output of the fuel cell power plant.

The cost of any of the above methods of storage/on-line generation of hydrogen depends on: (i) The hydrogen production rate, (ii) The service conditions - i.e., operating depth, temperature and (iii) The duration of service. The technoeconomics of hydrogen production for undersea applications are different from those for terrestrial applications because of the special requirements imposed by operating depth (pressure hull) and safety considerations.

II. OBJECTIVE

The objective of this report is to evaluate the relative merits of hydrogen storage/on-line generation methods for a 75W, 1 year-service Aquanautics hydrogen-oxygen fuel cell for deep ocean application. Specifically, it is intended to evaluate the advantages of the ALWATT hydrogen generator over other methods.

III. APPROACH

As indicated in section-II, the cost of hydrogen for the Aquanautics fuel cell is influenced by the operating conditions (i.e., ocean depth) and service duration. In this paper, we compare the unit costs of hydrogen by different methods, identify the pressure-hull requirements, if any, and comment on the preferred method for the Aquanautics SPE fuel cell.

IV. BACKGROUND

(a) Hydrogen requirement for Aquanautics fuel cell:

One mole of hydrogen produces 53.6 ampere-hours (AH) of electricity at 100% efficiency and this translates to 26.8kAH/kg and 2.4AH/liter (STP). Aquanautics has defined a hydrogen requirement of 696 ml/min (STP) for a 75 watt, one-year service fuel cell. Thus, the total annual hydrogen requirement for the fuel cell is about 366kl or 32.7kg(STP).

(b) Description of hydrogen storage/generation schemes:

The following methods were considered for hydrogen delivery to the fuel cell:

A: Hydrogen storage methods:
- (i) Compressed gas
- (ii) Cryogenic storage
- (iii) Metal Hydride Storage

B: On-line generation methods:
- (iv) Methanol reformer
- (v) Aluminum corrosion
- (vi) ALWATT cell

Details of the above hydrogen storage/on-line generation methods are provided in Appendix-1. Ammonia and hydrazine based methods of hydrogen generation were not considered because of corrosion and catalyst poison problems.

V. ANALYSIS

(a) Conditions of comparisons and format of results:

Comparison of different techniques (Table-2,3) for the storage and/or on-line generation and delivery of 696 ml/min (STP) of hydrogen for 1 year is made at an ocean depth of 0-10,000 meters. For each of the schemes, the following comparisons are made:

(i) The relative hydrogen contents on a weight as well as volume basis. These values exclude the weight and volume of the pressure hull, where needed.

(ii) The issue, whether a pressure-hull would be required or not is addressed.

(iii) The relative costs of the different schemes for the storage/generation of hydrogen are presented. The costs exclude pressure-hull cost.

We submit that the pressure-hull weight, volume and cost are marine structural engineering issues and should be addressed separately.

VI. RESULTS AND CONCLUSIONS

Table-2 gives a comparison of volume and weight requirements for hydrogen storage/generation alternatives. The values refer to storage on land and exclude pressure hull contributions.

(a) Relative ranking of methods of hydrogen storage/production:

From table-2 and table 3 the following relative ranking of the hydrogen storage/production methods is deduced:

Weight (%) hydrogen: Cryogenic storage = Methanol reforming > Aluminum corrosion > Calcium hydride > ALWATT >Transition metal hydride > Compressed gas

Density (g of hydrogen/cc): Aluminum corrosion > ALWATT> Calcium hydride > Methanol reforming > Transition metal hydride > Cryogenic storage > Compressed gas.

Cost ($/kg) including fuel and installation cost, and excluding pressure hull cost: Aluminum corrosion < ALWATT < Cryogenic storage < Compressed gas < Calcium hydride = Methanol reforming < Transition metal hydride

Raw material cost ($/kg) excluding installation and pressure hull cost: Cryogenic hydrogen = Methanol reforming < Aluminum corrosion < Compressed gas < ALWATT < Calcium hydride < Transition metal hydride

Details of the chemistry and associated discussion for assessing the cost are presented in Appendix-1.

(b) Preferred method:

The estimated weight and volume of hydrogen for the 75 watt, 1 year-service fuel cell is 366kl (STP) or 32.7kg as mentioned in (IV). From economics and safety points of view, an on-line generation method that does not require a pressure hull is preferred.

The following on-line hydrogen generation methods do not require a pressure-hull: (i) The ALWATT, (ii) The aluminum corrosion and (iii) The hydrolysis of calcium hydride. Of these, the hydrolysis of calcium hydride is the most expensive process, ALWATT ranks second and aluminum corrosion reaction is of the lowest cost. All the three methods are low temperature processes operable with sea water. They produce high purity hydrogen required for SPE-type fuel cell contemplated by Aquanautics. However, ALWATT is the only method that produces both hydrogen and electrical energy, and as such is the method of choice to supplement 25W to make up a 100W 1-year power source.

Of the on-line hydrogen generation processes that require a pressure hull, the methanol reformer has lowest fuel cost. However, the process requires heat to evaporate the methanol, for the generation of steam and to support the endothermic reaction. The waste heat from the SPE fuel cell may be used for the evaporation of methanol. However, the process heat and steam will have to be generated by combustion of methanol. The combustion process consumes about 10% of oxygen from the artificial gill. Also, the carbon monoxide in the hydrogen stream needs to be lowered to ppm level as it is a poison for the hydrogen electrode catalyst. However, if a phosphoric acid fuel cell or a molten carbonate fuel cell is planned then it is likely that all the required heat may come from the fuel cell and the hydrogen electrode would be more tolerable to higher carbon monoxide levels from the methanol reformer. Nonetheless, this process is of high cost and increases the total oxygen demand of an SPE fuel cell.

The transition metal hydride is costly on a one-time-use basis. However, the hydrogen absorption/desorption process is reversible and the cost of multiple use would be lower. The method requires heat for operation. The waste heat from the low temperature fuel cell is insufficient to support thermal decomposition. Hence is not attractive for the SPE fuel cell. Also, the method requires a costly pressure-hull housing and hence is not preferred.

Table-1
BASIS OF HYDROGEN GENERATION METHODS

Method	Storage/production Example/conditions	Basis
Compressed gas	High pressure storage	To conserve volume
Liquid Hydrogen	Special vessel Attrition: 1%/day	Cryogenic
Methanol	$CH_3OH + H_2O =$ $CO_2 + 3H_2$	Steam reformer
Metal Hydride	$CaH_2 + 2H_2O =$ $Ca(OH)_2 + 2H_2$	Reaction with water
	$FeTiH_2$ + Heat $FeTiH_x + x/2H_2$	Thermal decomposition
Metal	Al+alkali/salt water = Al salt + H_2	Corrosion
	Al + seawater = $Al(OH)_3$ + Electricity	Voltaic cell

Table 2
VOLUMETRIC AND GRAVIMETRIC COMPARISON OF HYDROGEN PRODUCTION ALTERNATIVES

PRODUCTION METHED	HYDROGEN CONTENT Weight %	Volume (g/cc)
1) Compressed gas (a)	1.5	0.018
2) Cryogenic Storage (a)	12.5	0.071
3) Calcium Hydride (b)	9.6	0.163
4) FeTiH2 (a)	1.8	0.096
5) Methanol Reforming (b)	12.5	0.150
6) Aluminum Corrosion (a)	10.3	0.279
7) ALWATT Cell (a)	9.8	0.264

a) Reference 2.
b) Alupower estimate.

Table-3

TECHNOECONOMIC COMPARISON OF DEEP OCEAN HYDROGEN PRODUCTION

STORAGE/PRODUCTION SCHEME	ON-LAND COSTS HYDROGEN ($/kg)	INVESTMENT	DEEP OCEAN COSTS PRESSURE HULL
Compressed Gas	10 (a)	12,000 (b)	Yes
Cryogenic Storage	6 (a)	16,000 (b)	Yes
Calcium Hydride (c)	243	-	No
$FeTiH_2$ (d)	700	-	Yes
Methanol Reforming	2 (e)	8000 (f)	Yes
Aluminum Corrosion (g)	30	-	No
ALWATT Cell (g)	214	-	No

(a) Commercial quote
(b) Annual rental cost of ground storage system
(c) Alupower estimate based on bulk cost of $23/kg.
(d) Reference 2.
(e) Alupower estimate based on $ 0.20/kg methanol
(f) Reference 4
(g) Alupower estimate based on internal costing.

VI. REFERENCES

1. "Handbook of Batteries and Fuel Cells", Ed., D.Linden.

2. B.V.Tilak, S.Srinivasan, T.C.Varljen and R.J.Pryputniewucz, Chapter 15, in Handbook of Energy Systems Engineering, Ed. L.C. Wilbur, John Wiley & Sons, Inc. 1985.

3. B.M.L. Rao and R.P. Hamlen, ECS Spring Meeting, Los Angeles, 1989, Abstract # 10.

1."Hydrogen: Production and Marketing", Ed., Smith and Santengelo.

APPENDIX-1

1. High pressure storage of hydrogen gas: This method of hydrogen gas storage is common where a relatively small quantities of hydrogen is required. Portable cylinders of hydrogen stored at 2400psi are used for laboratory purposes. Compressed gas cylinders (15-200 atms) are used in the larger scale distribution of gaseous hydrogen. As seen form Table-2 compressed gas hydrogen cylinders has the lowest hydrogen content both gravimetrically and volumetrically.

(ii) Cryogenic storage of liquid hydrogen: This is the preferred technology when large quantities of hydrogen must be stored or transported over long distances on land. This is probably the cheapest hydrogen storage alternative and the system hydrogen content is higher than Alwatt on a weight basis as seen from Table -2. The weight of cryogenic container for the Aquanautics annual requirement of hydrogen is estimated to be 260Kg. Although, this weight is less than that of ALWATT cell (400kg), the cryogenic container must be housed in pressure hull for a deep ocean application. The pressure hull adds to system weight, volume, cost and complexity. Also, there is additional penalty of about 1% evaporative loss per day in cryogenic storage of hydrogen and associated safety concerns. These issues render cryogenic hydrogen storage unattractive for Aquanautics use.

(iii) Metal hydride storage:

(a) Calcium Hydride: This is used as a reducing agent in the chemical industry. It has also been used as a source of hydrogen to fill reconnaissance and weather balloons. As indicated in Table-1, CaH_2 reacts with water to produce hydrogen and calcium hydroxide and the reaction can be used for on-line production of hydrogen. Like Alwatt, since the reaction involves sea water the calcium hydride storage would be an open system and no pressure hull would be required. For the Aquanautics annual requirement the weight of calcium hydride is estimated as 350 kg (based on 100% utilization) as compared to 400 kg for Alwatt. The corresponding volume of calcium hydride would be about 200 liters excluding the volume of the container. The system is relatively simple, however, at $23/kg of CaH_2 the cost of H_2 generation is $243/kg of hydrogen compared to the Alwatt cost of $214/kg.

(b) Transition metal hydrides: The principal of this method is that several metal, alloys and intermetallics absorb hydrogen under pressure forming the corresponding metal hydride and release the hydrogen when required on heating and lowering the pressure. The process is reversible and the average cost becomes less during multiple cycle use.

On a volumetric basis this method is superior to the cryogenic method but has considerable disadvantage on weight basis because of the weight of the associated metal. Heat and/or pressure swing is required for hydrogen generation. The waste heat from the SPE fuel cell is not sufficient to provide the process heat. It will have to supplemented by electric heating system or other by other means. This is a disadvantage of transition metal hydride method for Aquanautics use.

(iv) Methanol reformer: On a gravametric as well as volumetric basis there are distinct advantages of storing hydrogen in combination with other compounds (e.g. NH_3, $CO + 2H_2$ ---> CH_3OH). It would be cheaper to transport methanol than liquid hydrogen or metal hydride. However, the methanol reformer is good for a molten carbonate fuel cell and suffers from the following disadvantages for Aquanautics SPE fuel cell use:

(i) For an on-line delivery of hydrogen at a depth of 10,000 meters the methanol reformer will have to be in a pressure hull.

(ii) The capital investment for the reformer plant alone to meet the Aquanautics requirement is estimated to be $8000 based on mid-79 methane reformer plant costs. SPE fuel cell does not generate sufficient heat to generate steam and to operate the reformer. This heat requirement will have to be met with by methanol combustion using oxygen from the Aquanautics-gill source. This oxygen require. nt is estimated to be about 10% of the oxygen consumed by the fuel cell.

(iii) The hydrogen produced by methanol reformer contains trace CO, which is a poison for the fuel cell catalyst. The hydrogen from the reformer has to be purified.

(v) Aluminum Corrosion: In previous work, we have developed a hydrogen generator based on aluminum corrosion in the presence of alkali. We are in the process of developing a hydrogen generator based on salt water. As 18g of aluminum would produce 22.4 liters (STP) hydrogen in a simple reaction with salt water, this is an attractive approach to on-line hydrogen generation. This method does not require a pressure hull enclosure. However, the procedure is not fully developed and does not generate the supplemental electrical power as ALWATT cell.

(vi) ALWATT hydrogen generator: A complete Alwatt generator to meet the Aquanautics H_2 demand at 0 deg C and 1000 atm. would weigh approximately 100 kg and have a volume of 180 liters. (these values include 20% shunt correction). The cost of the generator as shown in the table does not include the cost of hydrogen recovery form the electrolyte and the associated pumping costs involved. We presume that pumping cost could be minimized by diverting the outlet stream from the oxygen concentrator into the ALWATT cell.

SECTION -II

ALWATT HYDROGEN GENERATOR POWER STUDY

ALWATT HYDROGEN GENERATOR POWER STUDY
AQUANAUTICS FUEL CELL

Shailesh Shah and B.M.L. Rao
Alupower Inc, 6 Claremont Road, Bernardsville, Nj 07924

I. INTRODUCTION

This is a computer modeling study of the relationship between power generated and the ALWATT™ system size, weight, operating depth and temperature. It is carried out to optimize the volumetric and gravimetric power densities of ALWATT at operating conditions varying from 0-10,000 meters ocean depth and 0-20 deg C. Specifically, the modeling is carried out for an ALWATT cell capable of delivering 25 watts together with a hydrogen production rate of 696 ml/min for 1-year as per Aquanautics directive (1).

II. POWER STUDY

Modeling of a parallel plate Alwatt cell that is open to sea water was done to determine the peak power densities with respect to weight and volume. The theoretical approach used is discussed below. The key data used were obtained from literature and laboratory results. They are discussed in Appendix-I.

(i) Optimization with respect to volume:

The power per unit volume obtained from an Alwatt battery is given as:

$$VPD = (E - IRL) * i * A * N / BV \quad \text{----------(1)}$$

where,
VPD = Volumetric Power Density (W/l)
E = Alwatt cell EMF (volts)
IRL = IR loss (volts)
i = Current Density (A/cm^2)
A = Cell Area (cm^2)
N = No of cells
BV = Battery volume (l)

Based on the equilibrium and kinetic equations for the hydrogen and aluminum half cells presented in the previous report (2) the relationship between the ALWATT emf and current density is derived in eq.-(2):

$E = 1.25+2.303RT/F*(0.06T-19.6-pH-\log(i^2)-1/2*(\log(P))) \quad -(2)$

where,

T = Cell Temperature,(deg K)

F = 96500 coul/eq,

pH = Electrolyte pH next to the hydrogen electrode,

P = Pressure (atm.)

The IR loss (IRL) encountered in the electrolyte gap is given as:

$IRL = i*R(T)*G \quad -(3)$

where,

R(T)= Electrolyte resistivity at temperature T (ohm-cm)

G = Cell Gap (cm)

The Battery volume can be calculated as:

$BV = (Alth + G) * A * N \quad -(4)$

where,

Alth= Aluminum thickness (cm)

Substituting equations (2), (3) and (4) in equation (1) we obtain:

$VPD = [(1.25 + 2.303\ RT/F * (0.06T - 19.6 - pH - \log(i^2) - 1/2\ \log(P) - i * R(T) * G) * i] / [Alth + G] \quad .... (5)$

A graphical solution of the above equation was sought and curves of power density versus current density were generated for different combinations of temperatures, pressures and initial and final (after discharge) cell gaps. These curves are presented in Figures 1 to 6.

<u>(ii) Optimization with respect to weight:</u>

For an ALWATT battery aluminum contributes to almost 95% of the total weight of the battery. The variation in the aluminum capacity (AH/g) is too small to have any incidence on the maximization of power with respect to weight. The variation in gravimetric power density (GPD) is shown by the following equation:

GPD = Power/weight

= (Cell E.M.F.)*(ALUMINUM CAPACITY)/(CELL ENDURANCE) ..(6)

III. RESULTS AND DISCUSSION

A. OPTIMIZATION OF VPD (W/kL).

(a) Effect of variation of initial gap of the cell:

Figure-1 and Figure-2 illustrate the varintion of VPD of the ALWATT cell with initial gap (0.1 to 0.5cm) operating at 20°C, 1 atmosphere and 0°C and 1000 atmosphere (atm). Figure-1 shows that the peak power density drops from 248 W/kl at 0.5 mA/cm^2 to 205 W/Kl at 1.5 mA/cm^2 when the initial cell gap increases from 0.1 cm to 0.5 cm at 20C, 1 atm. Similar effect of lowering of the power density with increasing initial gap is noted in Figure-2 for the low temperature and high pressure conditions.

(b) Effect of variation of temperature and pressure

Figure 3 and Figure-4 show that the VPD maximum occurs at 0.5 mA/cm^2 and 0.1 cm initial gap and is independent of temperature and pressure. However, the value of the maximum changes from 248 W/kl to 239 W/kl as the temperature decreases from 20° C to 0°C at 1 atm. (Figure-3). Similar results are obtained for the temperature dependence at operating pressures of 1000 atm. (Figure-4).

(b) Effect of increase in cell gap with depth of discharge:

The discussion that follows is for an ALWATT battery at its initial cell gap of 0.1 cm. It is important to realize that at 0.5 cm^2 the aluminum anode thickness is about 1.1 cm and as the aluminum is consumed during cell discharge the electrolyte gap increases form 0.1cm to 1.1 cm at the end for 90% utilization (external current + corrosion) of the anode. This increase in the gap with depth of discharge affects the maximum power that can be drawn, since the IR loss increases. The VPD dependence on current density at the end of discharge is shown in Figure-6 for cells with 0.1 cm initial gap. The results show that the peak power density remains at 0.5 mA/cm^2 at the end of diacharge and is independent of the temperature and pressure of operation.

B. OPTIMIZATION OF GRAVIMETRIC POWER DENSITY (W/kg)

The VPD of the cell is more sensitive to current density than the GPD. Therefore, it is appropriate to design the ALWATT cell based on the volumetric peak power and deduce the corresponding gravimetric power. For the conditions of maximum VPD discussed above, the gravimetric power density is 0.08 W/kg.

C. ENERGY DENSITY

The projected energy densities for a 25W, 1-year ALWATT cell operating at 0.5 mA/cm^2 and 0.1 cm initial gap, and for 0C, 1000 atm. conditions are 770WH/kg and 1796 WH/l based on initial conditions. Energy densities at the end of discharge are slightly lower (701 WH/kg and 1734 WH/l) due to increased gap from anode dissolution and consequential increase in IR loss.

D. BATTERY DESIGN

An example of a 6V, 25W, 1-year service battery incorporating shunt-loss compensation (three additional cells and shunt-fins) is presented in Appendix-II. The shunt-loss compensation used is based on other experiments has not been optimized for the ALWATT of this study. In comparison to the cell, the battery is about 25-30% lower in VPD, GPD and the energy density (Table-1) due to the method shunt-loss compensation used.

IV. SUMMARY AND CONCLUSIONS

(i) Maximum volumetric power for an ALWATT cell is obtained if the design is based on an operating current density of 0.5 mA/cm^2, and 0.1 cm initial gap, irrespective of the temperature or depth of operation. Under these conditions, the anode thickness is about 1.1 cm for 25W 1-year service.

(i) The operating conditions in (i) results in high energy density.

(iv) The numerical results for the cell and battery parameters at the end of discharge are of interest in assessing the ALWATT capability. This is summarized in Table-1.

TABLE-1

MAXIMUM POWER AND ENERGY DENSITIES AT END OF DISCHARGE
(1000 atm, 0C)

Parameter	Cell	Battery (*)
W/kl	198	138
W/kg	0.08	0.06
WH/Kg	701	534
WH/l	1734	1207

(*) Not optimized for shunt-loss compensation.

VI. REFERENCES

1. Discussions with Dr. Sam Mohanta

2. B.M.L. Rao and W. Halliop, 'Study of Hydrogen and Power Generation Characteristics of The ALWATT Underwater System', Submitted to Aquanautics Co, Dec 24, 1988.

Figure-1

POWER/VOLUME Vs CURRENT DENSITY

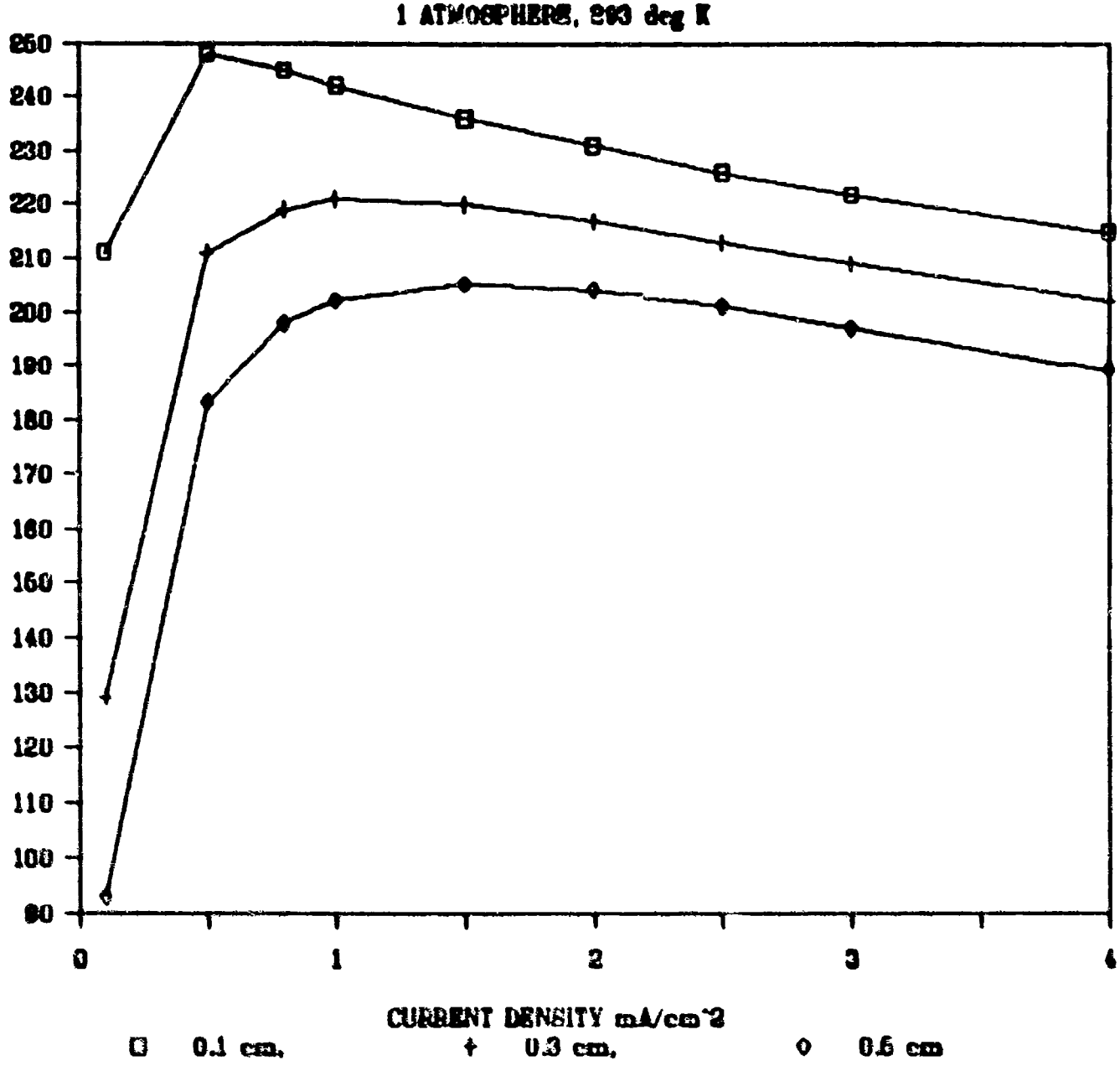

Figure-2

POWER/VOLUME Vs CURRENT DENSITY

0 deg C, 1000 ATMOSPHERE

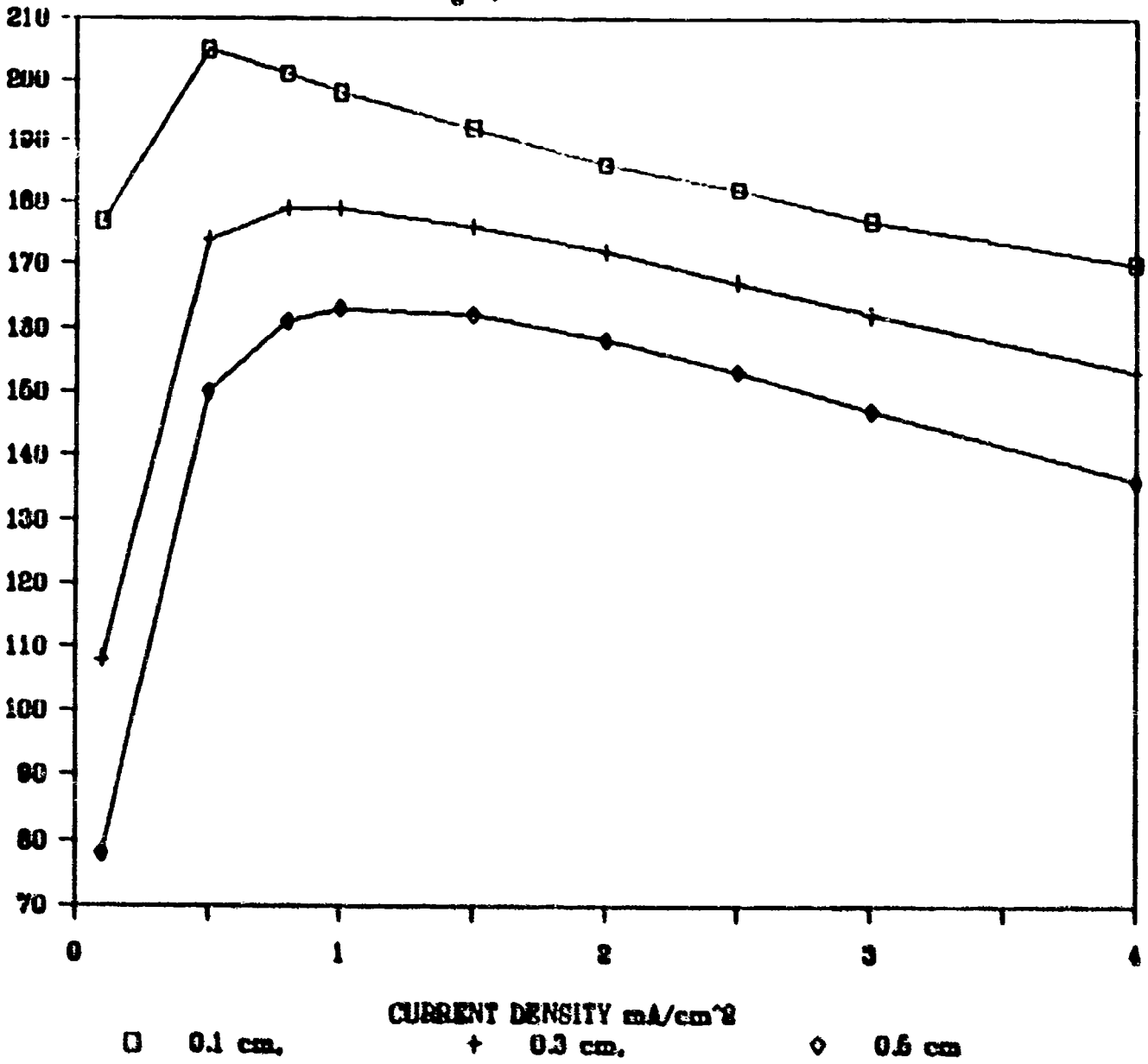

Figure-3

POWER/VOLUME Vs CURRENT DENSITY

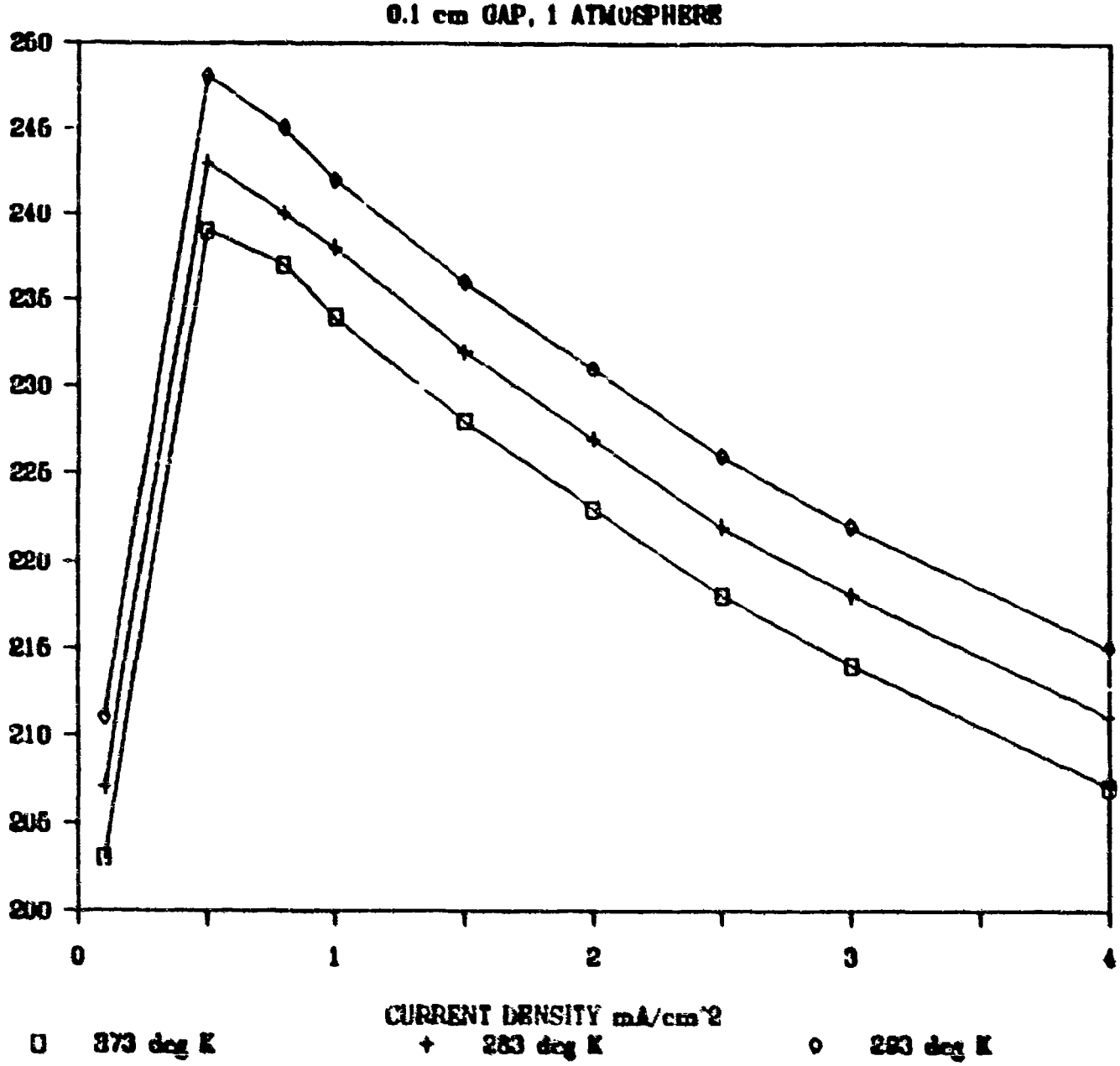

Figure-4

POWER/VOLUME Vs CURRENT DENSITY

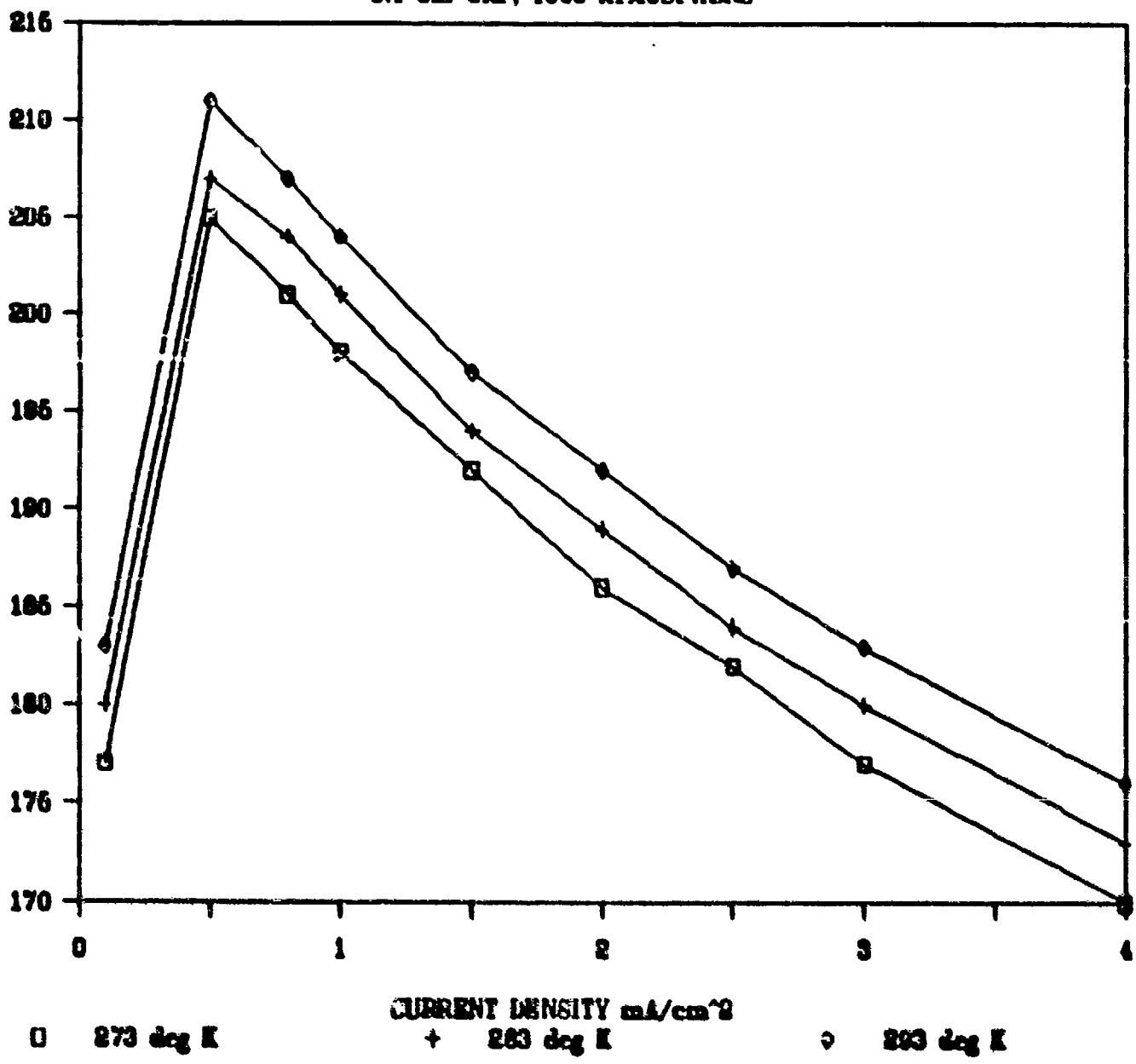

Figure-5

POWER/VOLUME Vs CURRENT DENSITY

1 ATM, 293 deg K, 0.1 cm INITIAL GAP

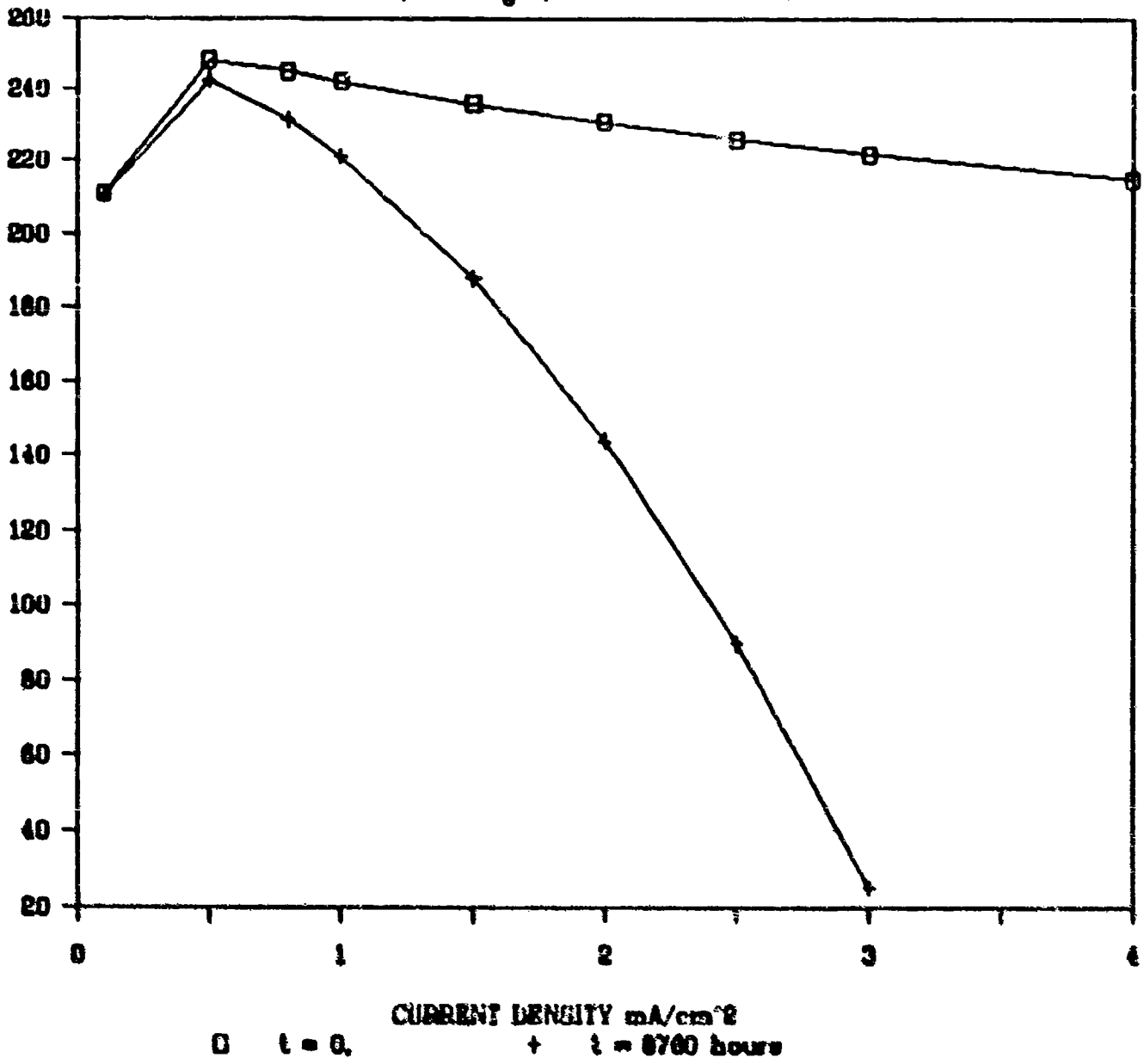

Figure-6

POWER/VOLUME Vs CURRENT DENSITY

1000 ATM. 273 deg K. 0.1 cm INITIAL GAP

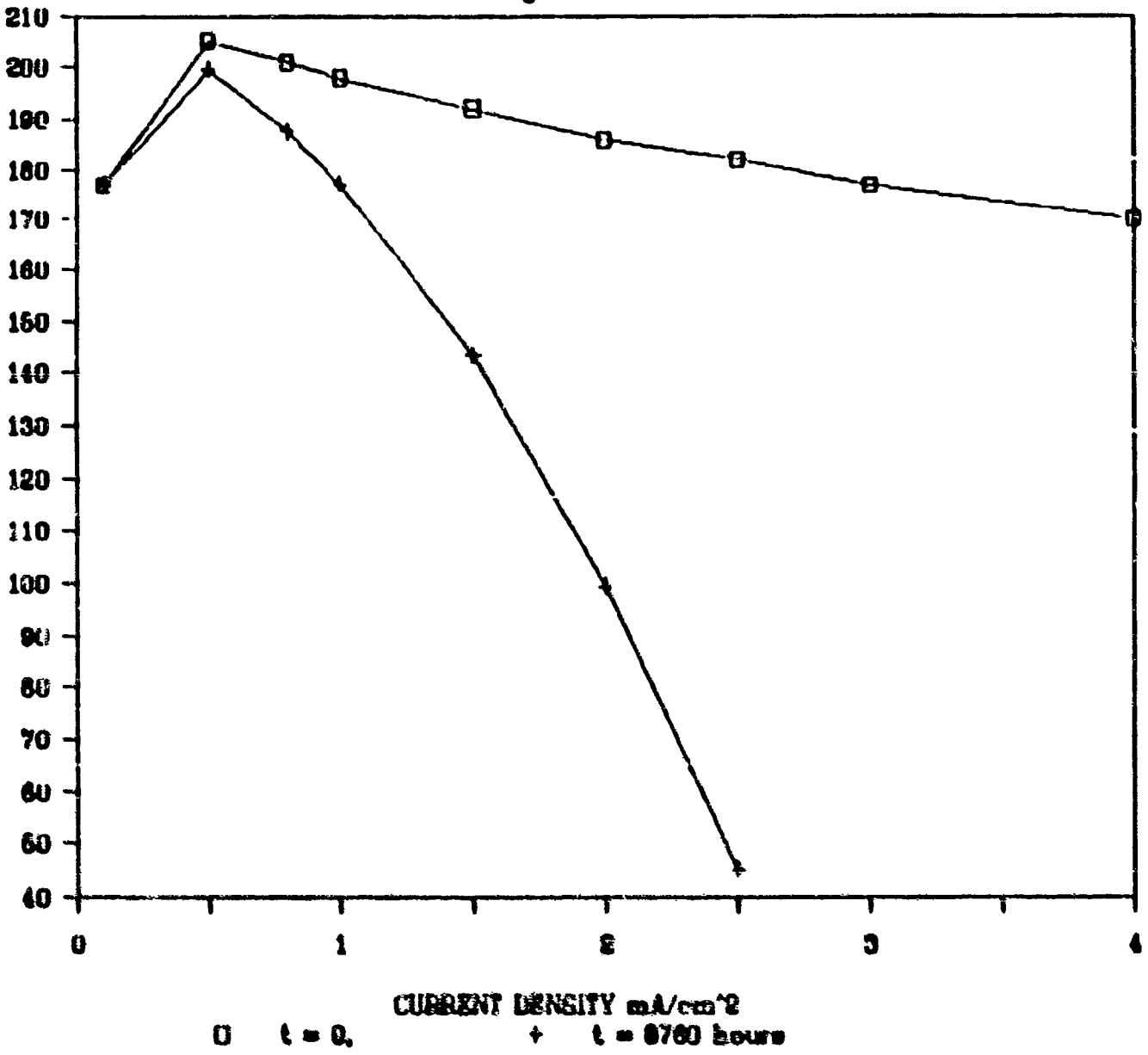

APPENDIX I

The following information was used in the optimization study

(i) Aluminum density ----------= 2.7 g/cc

(ii) Aluminum Capacity ----------= 1.5 AH/g
(value based on experimental results)

(iii) Aluminum half cell voltage -------= -1.25 vs NHE

As discussed in the previous report the half cell potential of Aluminum does not change significantly with the applied current over four decades from 0.1 mA/cm^2 to 100 mA/cm^2. Thus E_{Al} = -1.25 V vs NHE and is assumed to be independent of pressure and temperature in the region of Alwatt cell operation.

(iv) Alwatt exchange current density ---Log (i_o)= 0.03T-9.8

The above dependence of exchange current density on temperature was derived from literature data where T is in deg K and i_o is given in mA/cm^2. The pressure dependence of exchange current has been ignored because of uncertainty in literature data.

(v) Electrolyte pH----------= 10

The electrolyte pH next to the hydrogen electrode has been found to be equal to 10 due to the high concentration of OH^- ions there.

(vi) Electrolyte Resistivity:

The following values of the resistivity of 3% NaCl solution were obtained from literature:

0° C	=	38.34 ohm-cm
10° C	=	28.78 ohm-cm
20° C	=	24.85 ohm-cm

The pressure dependence of the ionic conductivity has been neglected.

APPENDIX-II

CONCEPTUAL DESIGN OF A 6 VOLT ALWATT BATTERY:

The following is an example of a 6 volt Alwatt battery capable of delivering 696 ml/min of hydrogen and 25 watts for 1 year. The design parameters including the shunt-loss compensation for the cell at the end of discharge are as follows:

1) Peak power density at 0° C, 1000 atm,(Fig-6)--- 198 W/kl

2) Corresponding Current Density ---------- 0.5 mA/cm^2

3) Aluminum thickness ---------- 1.08 cm
(0.0005 [A/cm^2]*8760 [H])/(1.5 [AH/g]*2.7[g/cc])

4a) Number of Cells before shunt compensation -- 13 cells
(6 [volts]/ .465 [volts/cell])

4b) Number of Cells with shunt compensation -- 16 cells

5) Initial cell gap ---------- 0.1 cm

6) Final cell gap ---------- 1.07 cm

7) Current ---------- ----------4.17 amps
(25 [watts]/(6 [volts]))

8a) Cell area at 0.5 mA/cm^2, (130*64.2 cm^2) ---- 8340 cm^2

8a) Cell area (130*72 cm^2 with shunt fins) ----- 9360 cm^2

9) Battery Volume with shunt compensation -------- 181.4 l
(9360cm^2]*(1.18[cm]*16cells]+ 0.5[cm,end plate thickness])

10) Battery weight ---------- 410 kg
(8340cm^2*1.08cm*2.7g/cc*16cells /0.95)

Appendix 2

Final Report

Fabrication of Aquanautics' Gill Membrane Module

AMT

FINAL REPORT

FABRICATION OF AQUANAUTICS' GILL MEMBRANE MODULE
P.O. #1360

The attached SECTIONS A - B - C constitute the entire Final Report representing the conclusion of Aquanautics' P. O. 1360.

SECTION A consists of Design Methodologies associated with fabrication procedures for the Artificial Gills. Both Gill Assembly and Potting procedures are described in Section A. All eight agreed upon Membrane Cartridges were fabricated per the design specifications shown. These Gill Cartridges contained 2.5 square meters and 1.0 square meters respectively, with the exception that two of the plasma coated units of Design #1 ended up approximately 5% less in total surface area.

SECTION B details the assumptions which go into a proprietary AMT Computer Model for commercial production scale, rough order of magnitude, price estimates. Using the coating method for AMT's Artificial Gill Membrane and automated assembly equipment for the Cartridges yields pricing estimates as shown in Section B. This Model also forms an integral part of the basis for development plans and projected development costs for Section C.

SECTION C details the overall development strategic objectives for scaling up Membrane Cartridge manufacturing under a world class manufacturing program, as well as the how-to's and tools needed to put such a program and facility into place over five years. Much of this framework is borrowed from Arthur Young and Company's National Director of Manufacturing Consulting Group, Thomas B. Gunn.

AMT has selectively incorporated Arthur Young and Company's recommendations which AMT believes to be relevant to getting its facilities of today up to production volumes suggested by Aquanautics - five years out. The largest costs are associated with capital equipment. Furthermore, the assumptions detailed in Section B are considered to form an integral part of Section C.

SECTION A

DESIGN METHODOLOGY FOR

MEMBRANE CARTRIDGE FABRICATION

MEMBRANE CARTRIDGE FABRICATION

The membrane cartridges were designed as a compromise between the desires of Aquanautics Corporation and the limitations of the available fabrication equipment. The mutually agreed upon design parameters are listed below:

DESIGN PARAMETERS FOR THE MEMBRANE CARTRIDGES:

Design Parameters	Design #1	Design #2
Fiber outer diameter	290 microns	290 microns
Length of Fibers	0.254 m	0.254 m
Thickness of Fiber Bed	25.4 mm	25.4 mm
Breadth of Fiber Bed	89 mm	89 mm
Inter-Fiber spacing	1.56 X OD	2.5 X OD
Total Surface Area Fibers	2.5 sq. meters	1.0 sq. meters

The membrane cartridges are designed to be of a cross flow design. Therefore the center section of each cartridge is open to allow fluid flow through the cartridge perpendicular to the fibers. The structure of the cartridges is illustrated in the attached drawing.

The fiber bundles were fabricated on a modified LaBlond metal turning lathe to provide control of the inter-fiber spacing. A fiber guide pulley was attached to the tool carriage and the screw thread cutting gears were engaged so that the tool carriage would move relative to the rotation of the chuck. The proper gears were engaged to give the desired fiber spacing. The setting of 56 turns per inch was used to achieve the fiber spacing factor of 1.56 X OD and 36 turns per inch was used for the fiber spacing factor of 2.5 X OD. A DC motor with speed controller was used to turn the lathe's chuck so that precise control of rotational speed could be maintained.

The fiber could not be pulled onto the winding fixture directly since the fiber tension needs to be carefully controlled. AMT's custom unwind stand was used to achieve uniform and controlled fiber tension. This fixure consisted of a series of pulleys and dancer arms through which the fiber was threaded. One dancer arm had a proximity sensor that sensed the position of the arm. The output of this sensor was used to control the speed of a stepper motor attached to the spool of fiber. The controls are set so that as fiber tension increases the unwind rate increases to decrease tension. AMT's fixture allowed the tension of the fibers to be controlled to levels of between 3 and 5 grams.

The winding fixture was designed to wind two cartridges at a time. The fibers are wound directly into the framework of the modules. The side rails and backside crossmembers are solvent bonded together to form an open U shaped channel. This framework is mounted onto a plate. Two of these plates are mounted back to back on a shaft held between the chuck and tailstock of the lathe. This shaft has a pulley attached that is driven by a DC motor.

The thread cutting feature on the lathe is used to control the spacing between fibers as each layer of fiber is wound. The spacing between each layer of fibers is controlled through the use of plastic spacers with pressure sensitive adhesive that also glue the fibers in place. These spacers are used on each end of the module and also on the two intermediate crossbars. The combination of the adhesive thickness and plastic material thickness yields the required inter-fiber spacing. At the ends of the cartridge the adhesive strips mount onto an aluminum strip with long screws. The strips are die cut with holes located to fit over these screws, These aluminum strips have short legs that index off of the end of the cartridge framework. This arrangement keeps the fibers located properly and under the proper tension when the cartridge is removed from the frame for potting.

The winding of the cartridge is accomplished by positioning the tool carriage so that the guide pulley is located at one side of the cartridge frame. The double sided adhesive strips are placed at the four locations (two ends and two in the middle) of each cartridge. The fiber is threaded through the unwind fixture and taped to the winding fixture. The DC motor is turned on slowly and the fixture is turned the proper number of turns to form one layer. Turns are counted with the use of a electronic counter that is activated by a cam and switch on the winding shaft. As the winding fixture turns the tool carriage traverses and the fiber is spaced out across the width of the cartridge. When a complete layer is formed, the winding is stopped and a layer of adhesive strips is put over the fibers in the four places mentioned above. The feed direction of the tool carriage is reversed and the next layer of fiber is wound. Since the gear train of the lathe has some backlash, the tool carriage does not start to traverse until the winding fixture has turned approximately one half revolution. This delay in starting the traverse back across the cartridge provides an offset in the fiber spacing between layers so that the fibers are staggered when viewing the fiber bundle front to back. This process is repeated over and over until the required number of layers is formed.

When the fiber bundle is formed, aluminum strips are placed on each end of the cartridges so that the adhesive strips are sandwiched between it and the bottom aluminum strip. The remaining pieces of the cartridge framework are bonded in place and then the fibers on each end are cut so that the two cartridges are independent. The cartridges are then removed for potting.

MODULE POTTING OUTLINE

This process outline applies to:

A. Potting of two modules at once.

B. Application of the 50 inch spinner arm.

PROCEDURE:

1. Inspect potting boats. Make sure that they are clean and intact. Replace if necessary.

2. Dip seal the fiber bundle with silicone RTV. This prevents the polyurethane from flowing into and plugging the fibers.

3. Apply a thin layer of silicone grease around the end of the module and insert it into the boat.

4. Screw a 10-32 x 1/8" barbed nylon elbow into the side of the boat.

5. Solvent bond two inches of 5/32"ID x 1/4" OD PVC tubing to one end of a three inch piece of 1/4" ID x 3/8" OD PVC tubing using cyclohexanone. To the other end, solvent bond a piece of 3/8" ID x 1/4" OD PVC tubing equal in length to the potting station distance on the spinner arm. Cut a small notch in the 3/8" OD tubing near the end bonded to the longer piece. This will allow air to escape from the line when glue is injected into the module. (Alternately, provide an overflow tube to the boat and utilize 5/32" ID x 1/4" OD PVC tubing for the entire tubing system).

6. Preheat the spinner machine by turning on the fan and setting the heater element at 175°F.

7. Secure the module and the tubing in the spinner arm channel with Aluminum Angle and Bunge cords. Two modules must always be spun at the same time. This will insure proper balancing of the system.

8. Next, prepare the polyurethane resin.

   The recipe calls for 54% Polycin 942 and 46% Vorite 689.
   For one module end, mix 86.4 grams of Polycin 942 with 73.6 grams of Vorite 689 in a 600 ml plastic beaker.

   For two modules, mix 86.4 grams of Polycin 942 with 73.6 grams of Vorite 689 in two 600 ml plastic beakers. Each module end should require about 80% to 90% of the resin to be properly filled. Mix thoroughly with a tongue depressor and degas the mixture in a vacuum dessicator under 29+ in Hg until bubbling ceases.

9. Cut a three inch piece of copper tubing with a tubing cutter and bend it to about a 120° angle. Fit the tubing onto the luer tip of a 20 cc syringe.

10. Pull the plunger and pour the degassed resin into the syringe while holding your finger over the end of the copper tubing. Re-insert the plunger and flip the syringe upright. Expel air from the syringe by depressing the plunger. (Steps 9 and 10 may be eliminated if you utilize an overflow tube).

11. Start the spinner and adjust RPM so that the module end has an acceleration of at least 150 g (Table 1). RPM can be checked with the strobe. The temperature in the spinner should be between 110°-115°F. Inject the resin into the top notch of the resin distributor in small volumes across a 3 to 5 minute span. It takes a small amount of time for the resin to evenly distribute around the fibers, and adding multiple small volumes will help prevent over-filling the module. The resin level can be monitored by observing the fill level in the clear resin addition tube. Inject resin into the bottom notch of the resin distributor and fill the second module in the same manner.

12. Fill in the module type, the starting temperature, the RPM's, and the starting time in the Log Book.

13. Continue to spin the modules for 90 minutes at 110° - 115°F to allow the resin to set.

14. Fill in ending time and temperature in the Log Book.

15. Remove the module from the spinner arm and allow the resin to set for 30 minutes at room temperature. Then remove the potting elbow from the boat and twist the boat off the module.

16. With the band saw, saw the end of the module off just below the score line. (1.5mm from the end) Make sure this step is done within 1 hour from the end of potting.

17. Cut through the polyurethane in one smooth cut with a razor blade.

18. Check the cut end of the module under the microscope to verify that the fibers are open properly.

19. Allow the urethane to set for 48 hours at room temperature or four hours at 60°C. The module is now ready for sealing on its endcaps and then for leak testing.

TABLE ONE

Rpm's required to attain 150g at each potting station along the 50 inch spinner arm:

$A_v = rw^2$

For max. = 730 rpm (12.2 rps)

$w = 76.3/sec$

$w^2 = 5826/sec^2$

R (in)	Rpm
11	693
13	638
15	594
17	558
19	527
21	502
23	479
25	460

SECTION B

PRICE ESTIMATES FOR PRODUCTION SCALE CARTRIDGES

ASSUMPTIONS INPUT SECTION	Year 1	Year 2	Year 3	Year 4	Year 5
Funding					
Funding Provided for Venture					
Sale Demand (Equal to Venture Output)					
AMT					
Property and Equipment Related					
Property & Equipment inflation Factor					
Number of Coating Machines					
Coating Machine Cost					
Capacity (sq.ft.per shift)					
Capacity Discount Factor					
Coating Method 1					
Number of Bundling Machines					
Bundling Machine Cost					
Other Equipment Additions					
Number of Machine Shifts					
Required Warehouse Space Per Machine (sq.ft)					
Cost of Warehouse Space (per sq.ft)					
Leasehold Improvement Additions					
Usefull Life of Equipment (years)					
Operating Costs Related					
Operating Costs Inflation Factor					
Fiber Cost					
Average Fiber Inventory					
Coating Costs (per sq.ft.)					
Coating Method 1					
Coating Mix					
Coating Method 1					
Scrap Factor					
Production Cost Markup (per sq.ft.)					
Encapsulating Cost (per sq.ft.)					
Method 1					
Encapsulating Mix					
Method 1					
Utilities (Porportions) w/# of Machines					
Gases (Per shift)					

WAGES AND EMPLOYEE BENEFITS	Year 1	Year 2	Year 3	Year 4	Year 5
Day Shift					
Operator #1					
Operator #2					
Operator #3 (When Coating Machines)=6)					
Operator #4 (When Coating Machines)=8)					
Operator #5 (When Coating Machines)=10)					
Quality Control/Winder					
Potter Operator #1					
Potter Operator #2 (When Bundler)=2					
Potter Operator #3 (When Bundler)=3					
Materials Handler					
Plant Manager					
Quality Control/Winder					
Night Shift					
Percentage of Day Shift Coating Operators					
Employee Benefits & Payroll Taxes (Addt'l)					
Insurance (Porportional w/# of Machines)					
Supplies (Porportional w/# of Machines)					
Miscellaneous (Porportional w/# of Machines)					
General and Administrative Cost Related					
General & Administrative Costs Inflation Factor					
Office Space Requirements (sq.ft.)					
Office Space Cost (per sq.ft.)					
Utilities					
Wages & Employee Benefits					
Office Manager					
Office					
Employee Benefits & Payroll Taxes (Add'l)					
Telephone					
Travel					
Professional Services					
Management Fees					
Miscellaneous					
Other Assumptions					
Average Accounts Receivable Days					
Average Accounts Payable Days					

CALCULATIONS SECTION (no input required)	Year 1	Year 2	Year 3	Year 4	Year 5
Total Funding					
Sales					
Sales Volume (sq.ft.fiber)					
AMT					
Sales Dollars					
AMT					
Fiber Cost Per Sq. Ft.					
Average Production Cost Per Sq. Ft.					
Average Profit Per Sq. Ft.					
Average Selling Price Per Sq. Ft.					
Property and Equipment Related					
Property and Equipment (AT Cost)					
Coating Machines					
Bundling Machines					
Other Equipment					
Production Capacity (sq.ft)					
Operating and G&A Cost Related					
Leased Space - Production					
- Office					
Purchased Fiber (dollars)					
Coating Costs					
Encapsulating Costs					
Gases					
Wages & Employee Benefits - Production					
- Office					

CAPITAL EQUIPMENT REQUIREMENTS

	YEAR 1 (403 K sq.ft)	YEAR 2 (2 MM sq.ft)	YEAR 3 (7½ MM sq.ft)	YEAR 4 (15 MM sq.ft)	YEAR 5 (20 MM sq.ft
CAPITAL EQUIPMENT INVESTMENT	$ 1,215,000	5,100,000	16,250,000	27,600,000	31,300,000
PRICE/SQ.FT. (Module basis)	9.57	8.14	6.90	5.88	5.00

S E C T I O N C

DEVELOPMENT PLAN FOR SCALING UP

GILL CARTRIDGE MANUFACTURING

1. MANUFACTURING SCALE-UP:

Strategic objectives: World class manufacturing facility/program scale-up to 20 MM ft^2/annum by implementing CAD, CAE, GT and CAD to CAM linkage, by improving product program management, by concurrent product and process engineering, by designing for (flexible) manufacturability, and by implementing standardized design procedures. - World Class Mfg. program -

Once the organization is put in place to administer implementation of the world class manufacturing program, it will be necessary to track and control the program implementation via project management software. There are many suitable personal computer-based project management control systems. It is essential that the software systems be capable of easily and quickly highlighting the critical path in the overall program at any given point. ("4th shift" is a highly recommended package).

STAGES

Initial

I. The initial stage (current-yr 1) can be characterized as follows: production set ups are exceedingly long - many hours in fact for both membrane and cartridge production.

- Annualized raw material and work in process inventory turns would amount to less than 6.
- Operations inefficiencies include inventory buffers, loosely coupled production, and excessive slack.
- Supplier involvement is present particularly for conceptual scale-up on membranes but not on the close basis needed long term. Little linkage at present to other suppliers, plastics, resins, metals, etc.

- Equipment preventive maintenance program needs to be installed - currently "fix it when it breaks" prevails.
- Total quality control program conceptually aware, but tools need to be put into place to implement same.
- The computing environment is batch. Many paper reports but little timely feedback on operations.
- Computing equipment is spotty. A few personal computers, and a few software packages.
- DataBase Management Systems and DATA processing capability are weak.
- CAD/CAE System use is not in place. Geometric part data on the drawings in both manual and computer codes. Part drawing still master part definition, ie. not integrated with business systems.
- Factory local networks data - collected on shop floor. No CNC controlled production equipment connected yet.
- All quality costs really not measured, probably 30%. Need to recognize necessity of four Feigenbaum Model costs
  - prevention
  - appraisal
  - internal
  - external
- Limited incoming sample inspections and material review committees utilized.
- Preventive maintenance education needed.
- Product and Process Design involvement as well as knowledge of TQC is very little. Education lacking in SQC, Taguchi Methods, and Quality Function Deployment.
- Role of Technology in attaining quality is primarily limited to mechanical gauges, dye testing, visual inspections and test fixtures, but some initial use of computers and software - driven process control/quality equipment installed. Software is utilized to capture quality data for analysis. Process monitors are programmable and could be readily automated.

II. Years 2 - Years 3

After considering all the how-do's and tools to implement in support of the manufacturing and business strategies (see appendix A) and a team of experienced personnel has been assembled into a planning task force, the specific manufacturing projects need to be identified, prioritized, scheduled and cost/benefits summarized. This should be done during Year one.

Project descriptions of this sort are extremely detailed and beyond the scope of this report, but a careful listing of all the assumptions which AMT considers important for world class manufacturing of its membrane cartridges are contained in the accompanying report dealing with projected rough order of magnitude product costs. This implementation stage of scale up to world class manufacturing status will be characterized by:

- Production set ups reduced in pilot attempts by at least 50%.
- Annualized raw material and work-in-process inventory turns move towards 12-15.
- Operations inefficiences attacked via established programs in many areas.
- Key suppliers involved to the point where inspectionless receiving can be started with some qualified suppliers.
- Equipment run at below rated speeds with workers in charge of light machine maintenance. Preventive maintenance structurally built in.
- Total Quality Control program implemented, tools in place and integration with JIT occuring.
- The computing environment includes daily batch updates, with on line inquiry status.
- Computing equipment proliferated thruout facility including relevant hardware, applications software, and telecommunication networks.
- Database Management Systems and DATA Processing Power (from work stations to MICROS) installed. Utilization of intelligent processing power from mainframes to MICROS to include DBMS and DATA dictionary use.

- CAD Systems used for drafting, and CAD/CAE Systems standardization emerging. Some CAD/CAE Systems used in design and analysis, work cell device programing. Electronic geometric part descriptions replace part drawing master part definitions. Technical computer systems integration with business systems initiated.
- Factory local area networks include CNC - controlled production equipment and DNC networks via MAP or proprietary networks attempted.
- Quality costs fully recognize all four Feigenbaum model costs. Costs as a % of sales reduced to 15-20%.
- Supplier certification for quality permits inspectionless receiving.
- Preventive Maintenance Program firmly established. Machines run at or below rated speeds.
- Teamwork established between product and process design.
- Role of Technology now expanded. Use of CAD/CAE in design, use of CIM technology and software to compare manufacturing process results with product and process design data.

III. YEARS 4 - 5

During this final phase of scale up the Company will progress to full implementation of JIT, full integration of CIM, and full connection/implementation of TQC.

- Production set ups reduced from original at least by 75%, some areas as high as 90% - many set up in minutes.
- Annualized raw material and work in process inventory turns 20-25 overall, 40-50 in some lines.
- Operations inefficiencies attacked in all programs, reductions widespread.
- 90% of suppliers certified for inspectionless receiving, number of suppliers reduced to minimum.
- Preventive maintenance a necessity of JIT and becoming fully practised.
- Total Quality Control program an equal partner of CIM and JIT.
- Computing environment on line interactive with real time updates.
- Computer equipment/electronic links to supplier/customers fully established.
- Several DBMS but one logical integrated DATABASE design with use of a standardized data dictionary.
- Geographic and hierarchical dispersion of intelligent processing power.
- CAD/CAE fully integrated for design and work cell device programming, electronically linked to bill of material and process/routing (MAP) and other business sytems.
- Fully integrated factory LAN using latest MAP specification or proprietary network for scheduling, quality, process control, preventive maintenance, and material movement.

- Quality costs as a % of sales reduced to 1 - 5%.
- Long term partnerships (sole sources) established for high quality suppliers.
- Product and process design requires design quality integrated with TQC.
- All employees trained in Design for Quality, Taguchi Methods, and SQC.
- Role of Technology (CIM) plays an inseparable role with people in promoting, measuring and ensuring quality.

Manufacturing Strategy Objective: ESTABLISH WORLD CLASS MANUFACTURING PROGRAM FOR ARTIFICIAL GILLS

Company Functions

How-to	Product Design Engineering	Information Systems	Manufacturing	Purchasing	Marketing	Human Resources	Quality Control	Accounting
1b Reduce cumulative manufacturing lead time *CIM tools *CAI *AGVS	*Design for manufacturability *Use Group technology to create part families	*Acquire CAI equipment *Link CAI equipment to mainframe *Establish quality data bases *Link CAD data to CAI equipment *Acquire statistical analysis and graphics tools *Establish FMS control network *Integrate FMS with MRP	*Specify and install FMS *Alter process plans for CAI *Re-layout plant for FMS *AGVS	*Reduce list of required raw materials	*Establish new order lead times	*Retrain displaced machinists *Educate FMS workers	*Select Q.C. steps amenable to vision inspection *Capture Q.C. data permently *Perform on-going analysis of Q.C. data for process control & preventive maintenance	*New cost justification methods for equipment *New overhead allocation procedures

Manufacturing Strategy Objectives: ESTABLISH WORLD CLASS MANUFACTURING PROGRAM FOR ARTIFICIAL GILLS

	Company Functions							
How-to	Product Design Engineering	Information Systems	Production	Purchasing	Marketing	Human Resources	Quality Control	Accounting
Apply JIT production techniques	*Design for manufac-turability	*Alter MP & CS logic *rate-based scheduling *smaller time buckets *backflush inventory relief *Electronic links to suppliers	*Freeze MPS *Sequence model production *Standardized containers *Eliminate waste	*Educate suppliers *Daily deliveries *Sole source purchasing *Closer suppliers *Improve supplier's processes, design and quality; reduce their costs; improve schedule compliance	*Realize customer product options effect on -product cost -manufac-turing complexity	*New overtime procedures *Train workers to be multi-functional *Educate all personnel about "JIT"	*Increased preventive maintenance *Andon signs *Bakayoke devices *Inspection-less receiv-ing	*Move toward total cost analysis *New overhead allocation procedure